JAERI-M
93-052

STATISTICAL THERMODYNAMIC PROPERTIES OF URANIUM HEXAFLUORIDE

March 1993

Tetsuzo ODA

日本原子力研究所
Japan Atomic Energy Research Institute

JAERI-Mレポートは，日本原子力研究所が不定期に公刊している研究報告書です。
入手の問合わせは，日本原子力研究所技術情報部情報資料課（〒319-11 茨城県那珂郡東海村）あて，お申しこみください。なお，このほかに財団法人原子力弘済会資料センター（〒319-11 茨城県那珂郡東海村日本原子力研究所内）で複写による実費領布をおこなっております。

JAERI-M reports are issued irregularly.
Inquiries about availability of the reports should be addressed to Information Division Department of Technical Information, Japan Atomic Energy Research Institute, Tokaimura, Naka-gun, Ibaraki-ken 319-11, Japan.

編集兼発行　日本原子力研究所
印　　刷　ニッセイエブロ株式会社

JAERI-M 93-052

Statistical Thermodynamic Properties of Uranium Hexafluoride

Tetsuzo ODA

Department of Fuel Safety Research
Tokai Research Establishment
Japan Atomic Energy Research Institute
Tokai-mura, Naka-gun, Ibaraki-ken

(Received February 15, 1993)

Statistical thermodynamic properties of uranium hexafluoride (UF_6) for extended temperature range are investigated using simulation techniques. As useful information 200 vibrational states are specifically tabulated, where these are shown in the order of population at a temperature of 300 K. Simulations of UF_6 ν_3 band contour were made in order to investigate the isotopic selectivity. These revealed that the real spectrum should be quasi-continuous feature heavily overlapped by a number of hot bands, while the selectivity should slightly depend on the absorption frequency. The present study would provide useful information for designing of the "Infrared Uranium Enrichment Monitoring System" for safeguards on a gas centrifuge type uranium enrichment plant, and for other fundamental analyses of infrared spectra.

Keywords: Uranium Hexafluoride, Statistical Thermodynamics, Population, Infrared Spectrum, Simulation, ν_3 Band Contour, Hot Band, Isotopic Selectivity, Safeguards, Enrichment, Centrifuge

JAERI-M 93-052

UF_6の統計熱力学的性質

日本原子力研究所東海研究所燃料安全工学部
小田　哲三

（1993年2月15日受理）

UF_6の統計熱力学的諸性質を広い温度領域にわたって計算し、特に200の分子振動準位についての結果は300Kの温度におけるポピュレーション順にテーブル化した。さらに、UF_6 ν_3バンドカンターについてのシミュレーションと同位体選択性についての評価を行い、これによると多数のホットバンドによる重畳の結果、スペクトルは準連続的な形状を示すが同位体選択性はわずかながら吸収波長に対して依存性を示すことがわかった。本研究は遠心分離ウラン濃縮プラントの保障措置を目的とした「光吸収濃縮度モニタシステム」の設計に不可欠な情報となるだけでなく、一般の赤外スペクトルの解析にも充分役立つ結果を提供するものである。

東海研究所：〒319-11　茨城県那珂郡東海村白方字白根2－4

Contents

目　　次

1. Introduction

Gas centrifuge type uranium enrichment plants are considered to be one of the most important facilities from the viewpoint of safeguards since they could produce nuclear weapons-grade highly enriched uranium (HEU) in short time periods; the sensitive advanced technology used in such facilities is, however, considered to have to be prevented from unlimited distribution from the viewpoint of international non-proliferation scheme, and also the operators wish to control the access to the cascade area even for safeguards inspection in order to protect the commercial secrecy.

In accordance with the point of view mentioned above, we have developed the "Infrared Laser Uranium Enrichment Monitoring System", which is to allow us to measure the uranium enrichment and/or to confirm the absence of HEU in the process gas even at the outside of the cascade area, namely without access to the area. This system is founded on the fact that an absorption spectrum of uranium-hexafluoride (UF_6) slightly changes with the isotope ratio of uranium in an infrared active band.

It will be necessary for design of this system to clarify some problems regarding spectroscopic phenomena; the purpose of the present report is twofold: First, we present some statistical thermodynamic properties of uranium-hexafluoride, which are indispensable for practical applications to analyses of the molecular vibration-rotation spectra. Second, we describe a hot-band problem, which may often complicate the spectroscopic analyses. In addition, we shall simulate UF_6 infrared spectra, and refer to the dependence of isotopic selectivity (single-photon cross-section ratio) upon absorption frequency.

2. Fundamental consideration

2.1 General

Now considering a polyatomic molecule including N nuclei, we need 3N coordinates to describe their motion: There are 3N degrees of freedom in the molecular system. Among them six degrees are appropriated to the translational and rotational motion of the molecule, therefore the vibrational motion has (3N-6) degrees of freedom. (For a linear molecule such as HCl and CO_2, however, there are (3N-5) vibrational

1. Introduction

Gas centrifuge type uranium enrichment plants are considered to be one of the most important facilities from the viewpoint of safeguards since they could produce nuclear weapons-grade highly enriched uranium (HEU) in short time periods; the sensitive advanced technology used in such facilities is, however, considered to have to be prevented from unlimited distribution from the viewpoint of international non-proliferation scheme, and also the operators wish to control the access to the cascade area even for safeguards inspection in order to protect the commercial secrecy.

In accordance with the point of view mentioned above, we have developed the "Infrared Laser Uranium Enrichment Monitoring System", which is to allow us to measure the uranium enrichment and/or to confirm the absence of HEU in the process gas even at the outside of the cascade area, namely without access to the area. This system is founded on the fact that an absorption spectrum of uranium-hexafluoride (UF_6) slightly changes with the isotope ratio of uranium in an infrared active band.

It will be necessary for design of this system to clarify some problems regarding spectroscopic phenomena; the purpose of the present report is twofold: First, we present some statistical thermodynamic properties of uranium-hexafluoride, which are indispensable for practical applications to analyses of the molecular vibration-rotation spectra. Second, we describe a hot-band problem, which may often complicate the spectroscopic analyses. In addition, we shall simulate UF_6 infrared spectra, and refer to the dependence of isotopic selectivity (single-photon cross-section ratio) upon absorption frequency.

2. Fundamental consideration

2.1 General

Now considering a polyatomic molecule including N nuclei, we need 3N coordinates to describe their motion: There are 3N degrees of freedom in the molecular system. Among them six degrees are appropriated to the translational and rotational motion of the molecule, therefore the vibrational motion has (3N-6) degrees of freedom. (For a linear molecule such as HCl and CO_2, however, there are (3N-5) vibrational

degrees of freedom.)

An XY_6 type spherical-top molecule such as UF_6, which belongs to the highly symmetrical O_h point group, has 15 normal modes of vibration since the number N of nuclei is seven. However, they have a two-fold and four three-fold degeneracies[1], and it is therefore sufficient to consider six different modes: $\nu_1,\ldots,\nu_6$. Schematic diagram of those fundamental modes are shown in Fig.1. These modes may be put into two categories; the stretching modes ν_1,ν_2,ν_3 and the bending modes ν_4,ν_5,ν_6. For UF_6 the formers lie in higher energy levels in the range from 0.066 eV to 0.083 eV while the latters lie in rather lower energy levels in the range from 0.018 eV to 0.025 eV[2].

On an absorption spectrum, for instance an infrared ν_j band, some transitions of the type $\nu_i + \nu_j - \nu_i$ are observed near the ν_j band according to circumstances. Those are called "hot-bands", which originate from the transitions from vibrationally excited states ν_i to upper states $\nu_i + \nu_j$. Since molecular vibration is generally not harmonic, the hot-band appears at the position slightly shifted from the ν_j band according to the anharmonicity of vibration, and also the relative intensity depends on both Boltzmann factor $\exp(-E_i/kT)$ and vibrational transition moment with a given vibrational quantum number.

Many appearance of hot-bands should bring about a great difficulty in a spectral analysis, since the overlapping would cause the observed spectrum to be complicated for such a purpose. For a heavy molecule, e.g. UF_6, some vibrational quantum levels lie to the extent of rather low energy as shown in Fig.2, hence most molecules should possess not ground but excited states at ambient temperature; the UF_6 population of the ground state is, in fact, only 0.4% at a temperature of 300K. Therefore an observed spectrum of such molecules should be mainly caused by the superposition of many hot-bands rather than by the "cold-band" that is a series of transitions from the vibrationally ground state.

2.2 Boltzmann distribution

In order to consider an infrared spectrum superimposed by hot-bands it is necessary to calculate the number of molecules on both vibrationally and rotationally excited states as a function of temperature.

The motion of a molecule would be generally classified into that of electrons and that of nuclei, and the latter also would be classified

into vibration and rotation with respect to the interaction between a molecule and a photon. Accordingly there should be three classes of energy level of interest in a molecular system; spectroscopically they are commonly observed in the region of ultraviolet/visible, infrared, and far-infrared/microwave respectively. Those motions are not independent on each other, but could be treated as individual in cases where the energy difference between those levels be much large. (This treatment is known as "Born-Oppenheimer approximation".)

Considering infrared spectra, the energy level of interest is referred to the vibration and rotation of a molecule; in the present work we calculate the thermal population of each state, assuming that their motion is independent on each other. This approximation might, however, make the result somewhat inaccurate especially for polyatomic molecules such as UF_6 since, for instance, it may take place that the amounts of vibrational energy are of the same order of magnitude as those of rotational energy; the perturbation effects will be discussed in the latter section.

The population P_i of molecules in thermal equilibrium is generally given by the Boltzmann distribution law

$$P_i = (\text{const.})\ D_i \exp\left(-\frac{E_i}{kT}\right) \qquad (1)$$

where D_i is the degeneracy (total statistical weight) of i-th state, E_i the energy, k Boltzmann's constant and T the absolute temperature. If P_i represents the fractional population, the proportional constant in Eq.(1) can be described by means of normalizing the equation: Considering the energy levels quantized, and setting the summation of P_i over all states equal to unity, then one can get

$$(\text{const.}) = \frac{1}{\sum_i D_i \exp\left(-\frac{E_i}{kT}\right)}$$

Here the denominator is usually called "partition function Z", namely

$$Z \equiv \sum_i D_i \exp\left(-\frac{E_i}{kT}\right) \qquad (2)$$

and one can then rewrite Eq.(1) as follows:

$$P_i = \frac{D_i}{Z} \exp\left(-\frac{E_i}{kT}\right) \tag{3}$$

As indicated in Eq.(2), Z is a function of temperature T, and physically represents the "effective" number of states.

The representation of D_i and E_i should be given according to the type of motion, namely vibration or rotation, and the summation Eq.(2) which defines the partition function can be analytically carried out in each case.

2.3 Vibrational state

We will describe formulas used for calculating the population of vibrational states in the present section.

On the vibrational mode, in addition to the six fundamentals as mentioned in 2.1, there are generally overtones $2\nu_i$, $3\nu_i$,..., and combination tones $\nu_i + \nu_j$, and so on, hence numbers of vibrational levels are existent consequently. The population on each vibrational level can be calculated by means of Eq.(3), and in this case E_i denotes the energy of i-th vibrational level; on the assumption that the molecular vibration were harmonic the energy E_i could be represent as a linear combination of the fundamental vibrations:

$$E_i = \sum_{\beta=1}^{6} v_{\beta i} E_\beta \tag{4}$$

where $v_{\beta i}$ is the vibrational quantum number of i-th state and E_β the harmonic energy of fundamental vibration β.

The degeneracy D_i in Eq.(3) should be represented by a product of statistical weights $g_{\beta i}$ of fundamental vibrations:

$$D_i = \prod_{\beta=1}^{6} g_{\beta i} \tag{5}$$

where the weight $g_{\beta i}$ is given according to β as follows:

$$g_{\beta i} = \begin{cases} 1 & \text{for } \beta = 1 \\ v_\beta + 1 & \text{for } \beta = 2 \\ \frac{1}{2}(v_\beta + 1)(v_\beta + 2) & \text{for } \beta = 3, 4, 5, 6 \end{cases} \tag{6}$$

The degeneracy D_i can be therefore simplified to

$$D_i = \frac{1}{16}(v_2 + 1)\prod_{\beta=3}^{6}(v_\beta + 1)(v_\beta + 2) \tag{7}$$

On the harmonic-oscillator approximation it is known that the summation Eq.(2) which defines the partition function can be analytically carried out to yield[1,3]

$$Z_v(T) = \prod_{\beta=1}^{6}[1 - \exp(-\frac{E\beta}{kT})]^{-d_\beta} \tag{8}$$

where $Z_v(T)$ denotes the vibrational partition function and d_β is the degeneracy of the fundamental vibration β, namely

$$d_\beta = \begin{cases} 1 & \text{for } \beta = 1 \\ 2 & \text{for } \beta = 2 \\ 3 & \text{for } \beta = 3, 4, 5, 6 \end{cases} \tag{9}$$

Combining the equations (3) through (9), one can then calculate the fractional population of any vibrationally excited state.

2.4 Rotational state

In the preceding section it has been shown on the vibrational state, and now let us refer to the rotational state. No attempt will be made in this section to consider that the molecular rotation would be influenced on any vibrational motion and that the interatomic distance would be changed by centrifugal stretching in rotation: The molecular rotation will be treated under a "rigid-rotor approximation". (In fact, their effects should be important on the analysis of high-resolution spectra, so that they will be discussed in the latter section.)

One can also calculate the fractional population of each rotational state by using Eq.(3). In a spherical-top molecule such as UF_6 the rotational energy E_J can be represented as same as a linear molecule[1]:

$$E_J = BhcJ(J + 1) \tag{10}$$

where B is the rotational constant, and h and c are Plank's constant and speed of light respectively, and J denotes the rotational quantum number.

The degeneracy D_J should be divided into two parts:

$$D_J = g_J \cdot \varepsilon_J \tag{11}$$

where g_J is the "space degeneracy" and ε_J the degeneracy arising from nuclear statistical weight. Since the angular momentum components of J, J-1,..., 0,..., -J times $h/2\pi$ would appear if an external field were applied, the space degeneracy g_J can be written by

$$g_J = 2J + 1 \tag{12}$$

The second factor in Eq.(11) should be calculated from the group theory; namely that will be precisely determined by the rotational species. However, in the case of a spherical-top molecule in which the spin of four or six nuclei equals to 1/2 ε_J may be approximately represented as indicated by Hertzberg[1]:

$$\varepsilon_J \simeq \frac{8}{3}(2J + 1) \tag{13}$$

It should be noted that this approximation would cause error in analysis of a high resolution spectrum with low-J values since Eq.(13) should be valid for only large-J.

Substituting Eqs.(10) through (13) for Eq.(5), the fractional population P_J of spherical-top molecules with rotational quantum number J is given by

$$P_J = \frac{8}{3} \frac{(2J + 1)^2}{Z_R(T)} \exp\left[-\frac{BhcJ(J + 1)}{kT}\right] \tag{14}$$

where $Z_R(T)$ denotes the rotational partition function, and for an XY_n spherical-top molecule that is given by[4]

$$Z_R(T) = [(2I_Y + 1)^n/\sigma] \sqrt{\pi} \left(\frac{Bhc}{kT}\right)^{-\frac{3}{2}} \exp\left(\frac{Bhc}{4kT}\right) \tag{15}$$

where I_Y is the nuclear spin of Y atom and σ the classical symmetry number. For UF_6 one takes $I_Y = 1/2$, $n = 6$, and $\sigma = 24$.

3. Population of uranium-hexafluoride

Some statistical thermodynamic properties of UF_6 were calculated using formulas as above described, and also the calculations for SF_6 were carried in order to make a comparison. The vibrational parameters and rotational constants used in the present calculation are listed in table 1, where the wave number ν_β of radiation are presented rather than the energy E_β of fundamental vibration; ν_β is related to E_β as

$$E_\beta = hc\nu_\beta \tag{16}$$

In following paragraphs we shall describe the results on the vibrational and rotational states respectively.

3.1 Vibrational state

3.1.1 Energy levels and the partition function

The schematic diagram of some lower vibrational energy levels has been shown in Fig.2, which was generated using Eq.(6). As indicated from this figure several energy levels of UF_6 lie under the energy of 0.025 eV, i.e. T = 300K, while any of SF_6 lies above that energy, and a number of UF_6 vibrational states lie in the region of rather lower energy. This reveals that most UF_6 molecules in thermal equilibrium at ambient temperature should be populated in vibrationally excited states.

That mentioned above could be described more quantitatively by considering the partition function. That is, as mentioned in 2.1, the partition function would provide a standard estimating the extent of population distribution, since this function represents an "effective degeneracy" determined by a temperature and type of motion, as seen in Eq.(3). Figure 3 shows the $Z_v(T)$-T relation for UF_6 and SF_6 expressed by Eq.(8), and reveals that the population distribution should be more extensive in UF_6 than in SF_6 at any temperature.

3.1.2 Vibrational population

Tables 2 and 3 give some statistical thermodynamic informations on lower vibrational states at a temperature of 300K, where the states are put in order of the population rather than the energy. As revealed from these tables, the population is not always larger in a lower than in a upper vibrational level. This is because the population is given as a

product of the degeneracy D_i and Boltzmann factor $\exp(-E_i/kT)$ in a given temperature, as seen in Eq.(1): An increase of energy reduces the latter factor while the former would in general increase with energy. (See the column of D_i in tables 2 and 3.) Indeed, as indicated in table 2, the population for UF_6 is smaller of the ground state (E_i= 0, D_i= 1) than of many other excited states.

That will be more clarified through illustrating the population $P_i(T)$ against the energy E_i for a given temperature; such relations are shown in Figs.4 and 5, from which it is revealed that UF_6 molecules are populated in considerably wide range of energy.

In addition, the populations $P_i(T)$ for some lower levels were calculated as a function of temperature T. Figure 6 presents the populations for UF_6 and SF_6 of 8 lower levels; it should be noted that many actual levels are omitted since they would heavily overlap with the curves already shown. (For instance, the population of the hot-state (000112) amounts to 0.9% at a temperature of 300K, as seen in table 2.)

It is interesting to compare the population distribution for UF_6 with that for SF_6; figure 6 indicates that the UF_6 population on the ground state markedly decreases with increasing of temperature and that the values become comparable on a number of vibrational states above a temperature of 200K. In contrast, the SF_6 population on the ground state decreases rather moderately and is superior to the other even at a temperature of 350K. This should, of course, originates from the distinction between their schemes of energy levels, as mentioned in 3.1.1.

Moreover, table 2 indicates that only 0.4% of UF_6 molecules exist in the vibrationally ground state at a temperature of 300K and that the fractional population is less than 1% for any hot-state and also that the sum up to 200 states amounts to still only 57%. These should lead that an infrared spectrum of UF_6 becomes so dense or quasi-continuous due to the appearance of many lines in the case of an observation at ambient temperature. Even at a temperature of 200K the ground state population for UF_6 amounts to still only 4.5%, and a number of hot-bands may therefore overlap with the "cold-band", which is series of transitions from the vibrationally ground state. Hence it is predicted tc be difficult to resolve rotational and more fine structure and to analyze such a spectrum under a conventional resolution.

By contrast, the ground state population for SF_6 amounts to 30% at a temperature of 300K and is much larger than the other, as shown in Fig.6.

3.1.3 Cumulative population distribution

The cumulative population distributions were calculated against energy at points of temperature from 50K to 300K. Figure 7 illustrates the lines which represent the fraction of UF_6 molecules having energy not greater than the energy E. It should be noted that the cumulative populations presented in tables 2 and 3 differ from those in Fig.7 since the states were put in order of the population rather than the energy in the tables.

3.1.4 Density of vibrational states

An attempt was made at describing the density of vibrational states. We shall give the computational approach used as follows: For a given energy E let G(E) be the summation over all vibrational states of energy less than or equal to E, namely

$$G(E) = \sum_{0<E_i<E} D_i \tag{17}$$

where D_i is the degeneracy of i-th state as represented by Eq.(7). Considering the number of vibrational states in the range of energy from E to E + dE, that is G(E + dE) - G(E), and with dE→0 we get

$$G(E + dE) - G(E) = \frac{dG}{dE} \cdot dE = g(E) \cdot dE$$

where g(E), as indicated, could represent the density of vibrational states, thereupon

$$g(E) = \frac{d}{dE} G(E) \tag{18}$$

Now the derivative of G(E) is strictly either zero or undefined for each value of E since G(E) is a step function which originates from the quantized energy level scheme. (Refer to, for instance, Fig.7.) However, since the vibrational level density is very high except in the lower energy region, G(E) may be assumed to be a "smooth" function; then we use the approximate function as

$$\ell nG(E) \simeq P_n(\ell nE) \tag{19}$$

where $P_n(x)$ is a polynomial, and we neglect terms of order higher than the sixth:

$$P_5(x) = a_0 + a_1x + a_2x^2 + a_3x^3 + a_4x^4 + a_5x^5 \tag{20}$$

Hence, for the density of vibrational states g(E), we can write

$$g(E) = \frac{P_5'(\ell nE)}{E} \exp[P_5(\ell nE)] \tag{21}$$

where P_5' represents the derivative of the polynomial P_5.

A least-squares fit was made to find the coefficients of P_5 in two regions, i.e. $200 \leq E \leq 2000$ cm^{-1}, and $2000 \leq E \leq 5000$ cm^{-1} since, in the lower energy region, the present approximation might be somewhat unrealistic due to the discrete feature of energy level. The results are presented in table 4, and the density of vibrational states for each molecule are shown in Fig.8, which were generated by use of Eq.(21).

3.2 Rotational state

The rotational populations in thermal equilibrium are shown for UF_6 and SF_6 in Fig.9 respectively, which were generated by use of Eqs.(14) and (15). Since heavy molecules such as UF_6 have very low values of rotational constants B (e.g. B=0.0555 cm^{-1} for UF_6 [2] and B=0.09111 cm^{-1} for SF_6 [5]), the populations should extend to levels with high rotational quantum numbers, as indicated from this figure.

In order to find the maximum of rotational population in a given vibrational state, regarding the rotational quantum number J as continuous, let us differentiate Eq.(14) by J, and let the obtained equation equal to zero and solve it in respect to J, then we get

$$J = \left(\frac{kT}{Bhc}\right)^{\frac{1}{2}} - \frac{1}{2} \tag{22}$$

At room temperature the maximum should be therefore presented around $J \cong 60$ for UF_6 and $J \cong 50$ for SF_6. As revealed from Eq.(14), the population even on J = 120 amounts to 20% of the maximum value for UF_6 at a temperature of 300K. (Meanwhile this fraction is only 3% for SF_6.)

Add to the extend mentioned above, each J-level would degenerate

into some-fold and this may be removed by various interactions, for example, high-order Coriolis perturbation, therefore those effects will result also a complicated rotational structure.

4. Accuracy

The inaccuracy might be caused by following two major factors in the present calculation.

a) Uncertainty of the values used for the frequencies of fundamental vibrations and for rotational constants.

b) The approximate model used in the present calculation.

In order to estimate the contributions of the above two factors on the error, we shall discuss with regard to the vibration and rotation respectively in the following.

4.1 Vibration

No systematic study was made of the error arising from the first factor, but the value of 1% or less was estimated for the vibrational population by comparing the present results to the other evaluated by use made of other set of the fundamental vibration frequencies (for instance, those reported by Classen et al.[6]).

It is difficult to estimate the contribution of the second factor. The present model considers only vibrational states and only first order term in the vibrational quantum number to define energy levels. The energy of i-th vibrational level, in fact, could not be represented by Eq.(4) and the discrepancy from the harmonic oscillator must be taken into account. Considering the anharmonicity, the equation (4) should be corrected in terms of anharmonic constants X as follows[2]:

$$E_i = \sum_\beta v_{\beta i} E_\beta + \sum_\beta X_{\beta\beta} v_{\beta i}(v_{\beta i} + d_\beta) + \frac{1}{2}\sum_\beta \sum_{j\neq\beta} X_{\beta j} v_{\beta i}(v_j + d_j) \qquad (23)$$

where d_β is given by Eq.(9). The anharmonicities of lower vibrational states are, however, generally so small (see, for instance, Ref.2 or 7) that the second and third terms in Eq.(23) are much small compared to the first harmonic term. Precise values of anharmonic shift are not known but, according to estimate, they are on the order of 10^{-4} eV[7]. Hence the anharmonic effect on the population may be relatively small compared to the first above discussed. (For the assignment of a

into some-fold and this may be removed by various interactions, for example, high-order Coriolis perturbation, therefore those effects will result also a complicated rotational structure.

4. Accuracy

The inaccuracy might be caused by following two major factors in the present calculation.

a) Uncertainty of the values used for the frequencies of fundamental vibrations and for rotational constants.

b) The approximate model used in the present calculation.

In order to estimate the contributions of the above two factors on the error, we shall discuss with regard to the vibration and rotation respectively in the following.

4.1 Vibration

No systematic study was made of the error arising from the first factor, but the value of 1% or less was estimated for the vibrational population by comparing the present results to the other evaluated by use made of other set of the fundamental vibration frequencies (for instance, those reported by Classen et al.[6]).

It is difficult to estimate the contribution of the second factor. The present model considers only vibrational states and only first order term in the vibrational quantum number to define energy levels. The energy of i-th vibrational level, in fact, could not be represented by Eq.(4) and the discrepancy from the harmonic oscillator must be taken into account. Considering the anharmonicity, the equation (4) should be corrected in terms of anharmonic constants X as follows[2]:

$$E_i = \sum_\beta v_{\beta i} E_\beta + \sum_\beta X_{\beta\beta} v_{\beta i}(v_{\beta i} + d_\beta) + \frac{1}{2}\sum_\beta \sum_{j\neq\beta} X_{\beta j} v_{\beta i}(v_j + d_j) \qquad (23)$$

where d_β is given by Eq.(9). The anharmonicities of lower vibrational states are, however, generally so small (see, for instance, Ref.2 or 7) that the second and third terms in Eq.(23) are much small compared to the first harmonic term. Precise values of anharmonic shift are not known but, according to estimate, they are on the order of 10^{-4} eV[7]. Hence the anharmonic effect on the population may be relatively small compared to the first above discussed. (For the assignment of a

spectrum, however, the anharmonicity should become important, of course.)

The density of vibrational states might be somewhat unrealistic especially in the lower energy region. This is because the energy level is generally quantized, therefore the scheme becomes discrete, while that would become quasi-continuous in the higher energy region. (See Figs.4 and 5.) The density should be, strictly, defined only as the average value for a given range of energy. For instance, a value of 0.364 is evaluated from actual counting of states for the range from 250 cm^{-1} to 500 cm^{-1}, while a value of 0.353 from the present model.

4.2 Rotation

The experimental value of the rotational constant B was 0.0555 ± 0.0002 cm^{-1} for UF_6[2] and 0.09111 ± 0.00005 cm^{-1} for SF_6[5]. If the precise value exist in the range of the margins of error, the contribution of the first factor on the error of rotational populations would be estimated to be 1% or less. This error, in fact, depends on both the rotational quantum number J and temperature T, and, for instance, a value of 0.4% would be estimated at the maximum population for UF_6.

In the present model the rotational energy was evaluated in assuming that molecular rotation would be "rigid" and independent on molecular vibration. However the rotational energy may be, in fact, corrected for the centrifugal distortion, and also the levels may be perturbed by various effects, e.g. Coriolis interaction.

For a non-rigid rotor, one has to add the stretching effect arising from the centrifugal force on the internuclear distance to Eq.(10); on the moment of inertia of the system as a customary expression[8]

$$E_J = BhcJ(J + 1) - DhcJ^2(J + 1)^2 \qquad (24)$$

where D, known as the centrifugal distortion constant, is a quantity that can be evaluated from spectral analyses. The minus sign means, understanding classically, that moment of inertia should slightly increase when a molecule is fast rotating.

Besides the molecular rotation may be influenced upon the vibration; the rotational constant B would differ from one vibrational state to another. We find, in fact, that the dependence is fairly well

represented by an expression of the type[1)]

$$B_v = B_e - \sum_\beta \alpha_\beta (v_\beta + \frac{d_\beta}{2}) + \cdots \qquad (25)$$

where α_β is called the vibration-rotation constant, in which the differences between the average moments of inertia on individual vibrational states are taken into account. Though the rotational constant should, in fact, change periodically during molecular vibration, the "effective" rotational constant B_v represents the average value, and B_e is the rotational constant corresponding to the equilibrium bond length. (It should be noted that the B_v-value never equals the B_e-value even on the vibrationally ground state; the difference $1/2\Sigma\alpha_\beta d_\beta$ would originate from the zero-point vibration.)

It would become important for analyses of rotationally resolved spectra to consider the effects discussed above, nevertheless the correction is estimated to be much small for the rotational population: For UF_6 and SF_6 the centrifugal distortion constant D would be on the order of 10^{-12} eV at the largest[9)], hence this effect on the rotational population may be negligible. Meanwhile, the constants α_β in Eq.(25) are also small and usually positive but sometimes negative with values on the order of 10^{-8} eV[3)]; in fact, the rotational constant differs from the upper to lower vibrational state on a value of 6×10^{-8} eV for UF_6[9)] and 2×10^{-8} eV for SF_6[10)] with the ν_3 transition. No effect arising from the rotation-vibration interaction may, therefore, influence on the rotational population.

According to estimate, it is assumed that the accuracy would depend only upon the values used for rotational constants, similar to that of the vibrational population.

The present calculation may be, of course, applied to the other spherical-top molecules (e.g. CH_4, MoF_6 and PuF_6) when their frequencies of fundamental vibrations and rotational constants were known. As above mentioned, the accuracy of those calculations are sure to depend only upon the uncertainties of the values adopted.

5. Infrared absorption spectra

The general situation of level populations for both vibration and rotation have been expressed in the preceding sections, where it has

represented by an expression of the type[1)]

$$B_v = B_e - \sum_\beta \alpha_\beta (v_\beta + \frac{d_\beta}{2}) + \cdots \qquad (25)$$

where α_β is called the vibration-rotation constant, in which the differences between the average moments of inertia on individual vibrational states are taken into account. Though the rotational constant should, in fact, change periodically during molecular vibration, the "effective" rotational constant B_v represents the average value, and B_e is the rotational constant corresponding to the equilibrium bond length. (It should be noted that the B_v-value never equals the B_e-value even on the vibrationally ground state; the difference $1/2\Sigma\alpha_\beta d_\beta$ would originate from the zero-point vibration.)

It would become important for analyses of rotationally resolved spectra to consider the effects discussed above, nevertheless the correction is estimated to be much small for the rotational population: For UF_6 and SF_6 the centrifugal distortion constant D would be on the order of 10^{-12} eV at the largest[9)], hence this effect on the rotational population may be negligible. Meanwhile, the constants α_β in Eq.(25) are also small and usually positive but sometimes negative with values on the order of 10^{-8} eV[3)]; in fact, the rotational constant differs from the upper to lower vibrational state on a value of 6×10^{-8} eV for UF_6[9)] and 2×10^{-8} eV for SF_6[10)] with the ν_3 transition. No effect arising from the rotation-vibration interaction may, therefore, influence on the rotational population.

According to estimate, it is assumed that the accuracy would depend only upon the values used for rotational constants, similar to that of the vibrational population.

The present calculation may be, of course, applied to the other spherical-top molecules (e.g. CH_4, MoF_6 and PuF_6) when their frequencies of fundamental vibrations and rotational constants were known. As above mentioned, the accuracy of those calculations are sure to depend only upon the uncertainties of the values adopted.

5. Infrared absorption spectra

The general situation of level populations for both vibration and rotation have been expressed in the preceding sections, where it has

been revealed that most UF_6 molecules should possess vibrationally excited states at ambient temperature due to the low-lying and close spaced levels, and also that the rotational population should extend to fairly high-J levels. In the present section we shall consider the complex energy level scheme and hot-band overlapping as described in the preceding sections by means of simulating the UF_6 ν_3 band spectra.

An infrared spectrum originates from a transition between vibrational levels with a change of dipole moment, and the transition can be in general accompanied by a change of rotational quantum number. In order to simulate a spectrum it should be necessary to consider both frequency and intensity of the transition; the absorption frequency corresponds to the difference between the amounts of energy before and after the transition, and the intensity is connected with the transition probability.

5.1 Infrared absorption frequency

A transition from a state to another occurs generally in consistency with an appropriate selection rule. For a change of rotational quantum number J that is $\Delta J = 0, \pm 1$ in the case of a spherical-top molecule such as UF_6 and SF_6; a series of transitions accompanied with $\Delta J = -1$ are called "P-branch" and similarly "Q-branch" for $\Delta J = 0$, and "R-branch" for $\Delta J = +1$ (see Fig.10).

The transition frequencies in a dipole-active (infrared) fundamental of a spherical-top molecule can be expressed in the diagonal approximation as[10,11]

$$P(J) = m - nJ + pJ^2 - qJ^3 + gP_4 \tag{26}$$

$$Q(J) = m + pJ(J + 1) - 2gQ_4 \tag{27}$$

$$R(J) = m + n(J + 1) + p(J + 1)^2 + q(J + 1)^3 + gR_4 \tag{28}$$

with off-diagonal terms and diagonal sixth rank tensor terms in Hamiltonian neglected. In these equations J denotes the rotational quantum number before the transition, and the parameter m, n, p, q, g are molecular constants, which means the followings respectively:

m : the band center frequency

$n = 2B(1 - \zeta)$ (ζ is the Coriolis constant)

p : the effective change in the rotational constant, ΔB

q = -4D (D is the centrifugal distortion constant)

g : the octahedral splitting constant

, and the last terms in Eqs.(26) through (28) represent the fine-structure due to octahedral level splitting arising from perturbations, e.g. high order Coriolis interaction.

If the molecular vibration would be perfectly harmonic, the band-center m of any hot-band should be consistent with that of the cold-band, but actually the position is slightly shifted to the low frequency side due to the anharmonicity. Considering the ν_3 transition, the amount of energy m for $\Delta v_3 = 1$ would be expressed by

$$m = E_3 + X_{33}(2v_3 + 4) + \frac{1}{2} \sum_{j \neq 3} X_{j3}(2v_j + d_j) \qquad (29)$$

using Eq.(23), where the degeneracy of the ν_3 mode is 3. On the cold-band where $v_\beta = 0$, we get

$$m_0 = E_3 + 4X_{33} + \frac{1}{2} \sum_{j \neq 3} X_{ji} d_j \qquad (30)$$

where m_0 is the band-center of the cold-band. Comparing Eq.(29) with Eq.(30), we can get

$$m = m_0 + 2X_{33}v_3 + \sum_{j \neq 3} X_{j3}v_j \qquad (31)$$

where it should be noted that vibrational quantum numbers v's denote the value in the lower state.

In the present work we simulated relatively low resolution spectra as obtained by a conventional spectrometer in order to consider the heavy overlapping of hot-bands, hence the last terms in Eqs.(26) through (28) were neglected since the fine-structure would appear only at a fairly high resolution. In fact, the extent of this splitting is estimated to be on the order of 0.1 cm^{-1} from the g-value[10] and the diagonal $F^{(4)}$ coefficients of Moret-Bailly[12] for spherical-top molecules[13,14], though the octahedral splitting should depend upon the total angular momentum quantum number J.

5.2 Infrared absorption intensity

The absorption intensity for a given transition will be proportional to the population before the transition. The population P(v,J) on a given ro-vibrational level should be represented by a product of the vibrational and rotational populations; namely

$$P(v, J) = P_v \times P_J \tag{32}$$

where P_v and P_J have been already described. For a given P-, Q-, or R-branch transition, the intensity will be also proportional to an intensity factor θ(J), that is,

$$\theta(J) = \begin{cases} \dfrac{2J-1}{2J+1} & \text{for P-branch} \\ 1 & \text{for Q-branch} \\ \dfrac{2J+3}{2J+1} & \text{for Q-branch} \end{cases} \tag{33}$$

Furthermore, the intensity must be corrected by a stimulated emission factor,

$$[\ 1 - \exp(-\frac{hc\nu}{kT})\ ]$$

From the above discussion, the absorption intensity I_0 at a frequency ν_0 may be described as

$$\begin{aligned} I_0 &= C\ [\ 1 - \exp(-\frac{hc\nu}{kT})\ ]\cdot\theta(J)\cdot P(v, J) \\ &= C\ [\ 1 - \exp(-\frac{hc\nu}{kT})\ ]\cdot(2J_f + 1)(2J_i + 1)\cdot \\ &\qquad \cdot\exp[\ -\frac{BhcJ_i(J_i + 1)}{kT}\cdot Pv \end{aligned} \tag{34}$$

where C is an adjustable constant, and the subscript f on J indicates the final state and i is the initial state of the rotational level.

5.3 Spectral simulation

Now we can simulate a spectrum overlapped by a number of hot-bands at a given temperature, by combining the equations described in the

preceding paragraph with the results calculated in 3.1. However a spectrum observed actually will not be in a line type such as δ-function but in another profile due to distortions by various perturbations, which cause shifts in the effective energy levels with respect to the rest frame of an observer: An absorption line will become broadened over some extent of frequency region. Moreover the band spectrum may show a continuous distribution due to overlapping of a number of broadened rotational lines according to a resolution of a spectrometer used.

Under a high resolution the primary processes which cause a line-broadening should be

a) natural broadening

b) Doppler broadening

c) pressure broadening

, while the broadening arising from the performance of a spectrometer would become to dominate in decreasing a resolution. It is necessary for simulating an actual spectrum to calculate the intensity distribution over a given region of frequency; in the present work we should make a low or medium resolution spectrum in order to assess the hot-band overlapping over the whole band, therefore we assumed a Gaussian instrument function with a full-width at half-maximum (FWHM), namely

$$I(\nu) = I_0 \exp\left[- 4\ell n2 \frac{(\nu - \nu_0)^2}{\delta} \right] \qquad (35)$$

where δ is the FWHM, and ν_0 denotes the line center.

In order to simulate the hot-band overlapping accurately as possible the number of vibrationally excited levels was taken into account so adequately as the total population should amount to more than 99%, except for the case of a temperature of 300K on UF_6, where the value was no more than 97% even when the 3000 levels were taken into account. That is, UF_6 molecules are to be populated over considerably extent levels at such a temperature, as indicated in Fig.4 or 7. For the rotational level the number could be taken into account so sufficiently as the total population would amount to almost 100%, namely 200 levels at largest.

The molecular constants used in the present simulation are shown in table 5. In absence of measured values for anharmonicity, however, we

assumed that the anharmonic shift for a given vibrational band would be proportional to the energy for the lower level, namely

$$X_{j3} = -A\nu_j \tag{36}$$

where the constant A is an empirical parameter, and we used A = 1.28 x 10^{-3} for excited bending modes of UF_6[9].

Spectral simulations were made of the ν_3 band of UF_6 and SF_6 with variation in both temperature and FWHM. Figures 11 through 16 present the computer-generated spectra.

At a medium or low resolution, since each absorption line broadens and overlaps with other lines as mentioned already, an observed spectrum would become continuous and the rotational structure could not be resolved, though the profile has well-resolved P, Q, and R branch envelopes, as seen in the present results. Especially the contour of Q-branch region, which is the highest envelope appearing in the center of each spectrum, should become narrow and high due to the fact that an interval between adjacent lines is much close in comparison with that of the other branch, as revealed from Eqs. (26) through (28); hence the rotational structure could not be resolved for the Q-branch even under a fairly high resolution.

It is interesting to look over a change of the band contour with temperature; figures 11 and 12 reveal that the region of each branch becomes broadly and also that the highest position of Q-branch shifts to left-hand (low frequency side) with increasing of temperature. That is because the hot-bands appearing on a UF_6 spectrum grow in number with increasing of temperature, and because the anharmonicity increases with the amount of energy of the level. (It should be remembered that the anharmonic constants are all negative.) Meanwhile, for SF_6, figures 14 and 15 reveal that the Q-branch hardly shifts in a change of temperature and that a hot-band Q-branch shoulder arising from the transition $\nu_6 + \nu_3 - \nu_6$ appears distinctly at the left-hand side; in the case of SF_6 only several hot-bands contribute to the spectrum even at a temperature of 300K, hence the highest Q-branch envelop originates nearly only from the cold-band.

As revealed from a comparison between Fig.11 and Fig.13, it should be noted that an improvement of resolution could not change the

situation of hot-band overlapping on the UF_6 spectrum. This is because, in addition to many appearances of absorption lines, the anharmonic shifts are much small for lower-lying levels (see table 5). By contrast, figure 16 indicates that an increase of resolution distinguishes each hot-band and that the width also becomes narrow corresponding to the resolution for the SF_6 spectrum.

It is obvious that the ν_3 absorption band of UF_6 cannot be isotopically resolved under a medium or low resolution, since the isotope shift of 0.6 cm^{-1} has been found for $^{235}UF_6/^{238}UF_6$[2,15]. It is however anticipated that the isotopic selectivity depends on the absorption frequency. Figures 17 and 18 show such dependences generated by a simulation method, and, as indicated, the maximum points of the selectivity $\alpha(235)/\alpha(238)$ are shifted to the low frequency side, compared with the highest positions of absorption spectra: The maxima are situated at the right-hand slope of Q-branch envelope.

No attempts were made of simulating UF_6 spectra under a fairly high resolution and/or a fairly low temperature in the present work. In recent years Doppler-limited rotationally resolved spectra have been recorded for many kinds of molecules with a tunable diode laser (TDL) spectrometer and the other advanced techniques, which provide a greatly improved resolution of better than 10^{-3} cm^{-1}, and the octahedral fine splitting structures, as represented by the last terms of Eqs.(26) through (28), are observed on spectra for several kinds of spherical-top molecules (T_d or O_h point group) at a fairly low temperature[15-18]. The advanced techniques as mentioned above have provided detailed and accurate informations on a molecular structure, and have also demanded a theory appropriate to such fine spectra.

Though it is estimated to be difficult to obtain spectroscopic data detailed under ambient temperature due to the interference of hot-band overlapping, as discussed already, it might be possible that somewhat discrete features are observed under a fairly high resolution even at room temperature. (Those spectra should be, of course, still heavily overlapped with hundreds of hot-bands.) The work on such spectra will be reported on elsewhere.

6. Summary

Some statistical thermodynamic properties for UF_6 and SF_6 were evaluated from a data set of only fundamental frequencies and rotational constants. The present results should provide indispensable informations for the design of the "Laser Uranium Enrichment Monitoring System" and for basic analyses of infrared spectra. The present method also can be applied to the other spherical-top molecules such as PuF_6 and MoF_6.

As revealed from the present spectral simulation, the ν_3 band of UF_6 is expected to show quasi-continuous feature due to the overlapping of a number of absorption lines arising from the following facts: First, there is not much to choose among a number of vibrational levels for population due to the low-lying and highly degenerate energy level scheme. Second, the rotational population for UF_6 extends over a wide range of J-level due to the very small rotational constant.

References

1) Hertzberg G.: "Molecular Spectra and Molecular Structure, II Infrared and Raman Spectra of Polyatomic Molecules", van Nostrand Reinhold, New York (1945).
2) McDowell R.S., Asprey L.B., and Paine R.T.: J. Chem. Phys., 61, 3571 (1974).
3) Eerkens J.W.: U.S. Air Force FTD-CW-01-01-74 (1973).
4) Fox K.: J. Quant. Spectrosc. Radiat. Transfer, 10, 1335 (1970).
5) Berger H., Aboumajd A., and Saint-Loup R.: J. Phys. Lett., 38, L373 (1977).
6) Classen H.W., Goodman G.I., Holloway J.H., and Selig H.: J. Chem. Phys., 53, 341 (1970).
7) Cahen-de Villardi J., Clerc M., Isnard P., and Weulersse J.M.: J. Molecul. Spectrosc., 84, 319 (1980).
8) Dodd R.E.: "Chemical Spectroscopy", Elsevier Publishing Company, Amsterdam (1962).
9) Krohn B.J., and Kim K.C.: J. Chem. Phys., 77, 1645 (1982).
10) Galbraith H.W., Patterson C.W., and Krohn B.J.: J. Molecul. Spectrosc., 73, 475 (1978).
11) McDowell R.S., Galbraith H.W., Cantrell C.D., Nereson N.G., and Hinkly E.D.: ibid., 68, 228 (1977).
12) Moret-Bailly J.: ibid., 15, 344 (1965).
13) Krohn B.J.: ibid., 68, 497 (1977).
14) Krohn B.J.: LA-6554-MS (1976).
15) Takami M., Oyama T., Watanabe T., Namba S., and Nakane R.: Jpn. J. Appl. Phys., 23, L88 (1984).
16) Kim K.C., Person W.B., Seitz D., and Krohn B.J.: J. Molecul. Spectrosc., 76, 322 (1979).
17) Takami M., and Kuze H.: J. Chem. Phys., 80, 5994 (1984).
18) Kim K.C., and Briesmeister R.A.: LA-UR-83-1568 (1983).
19) Aldridge J.P., Brock E.G., Filip H., Flicker H., Fox K., Galbraith H.W., Holland R.F., Kim K.C., Krohn B.J., Magnuson D.W., Maier W.B., McDowell R.S., Patterson C.W., Person W.B., Smith D.F., and Werner G.K.: J. Chem. Phys., 83, 34 (1985).
20) Pine A.S., and Patterson C.W.: J. Molecul. Spectrosc., 92, 18 (1982).
21) Aboumajd A., Berger H., and Saint-Loup R.: ibid., 78, 486 (1979).

22) McDowell R.S., Aldridge J.P., and Holland R.F.: J. Phys. Chem., 80, 1203 (1976).

23) Pine A.S., and Robiette A.G.: J. Molecul. Spectrosc., 80, 388 (1980).

24) Person W.B., and Kim K.C.: J. Chem. Phys., 69, 2117 (1978).

Table 1 Fundamental frequencies and rotational constants[a)]

Molecule	ν_1	ν_2	ν_3	ν_4	ν_5	ν_6	B
UF_6	668.2[b)]	534.5[c)]	627.7[d)]	187.5[e)]	201[f)]	143[f)]	0.0555[f,g)]
SF_6	774.5[h)]	643.4[i)]	948.0[j)]	615.0[k)]	523.5[i)]	347.0[i)]	0.09111[i)]

a) All values are in cm^{-1}
b) Cahen-de Villardi et al. (7), as remeasured by Aldridge et al. (19)
c) Mean of measurements in Ref.(2) and Ref.(7)
d) See Ref.(19)
e) McDowell et al.(2), as remeasured by Aldridge et al. (19)
f) See Ref.(2)
g) Determined by band-contour analyses and data from electron diffraction; Aldridge et al.(19) give B = 0.05567 cm^{-1} from tunable diode laser spectra
h) See Ref.(20)
i) See Ref.(21)
j) See Ref.(10)
k) See Ref.(16)

Table 2 Calculated hot-state populations at 300K and statistical thermodynamic informations for UF_6

NO.	V1	V2	V3	V4	V5	V6	E(EV)	DH	SHIFT	POPULATION	CUSUM
1	0	0	0	1	1	2	0.08363	54	-0.82	9.0188E-03	9.0188D-03
2	0	0	0	1	1	1	0.06590	27	-0.65	8.9533E-03	1.7972D-02
3	0	0	0	1	0	2	0.05871	18	-0.57	7.8832E-03	2.5855D-02
4	0	0	0	1	0	1	0.04098	9	-0.40	7.8259E-03	3.3681D-02
5	0	0	0	1	1	3	0.10136	90	-0.99	7.5707E-03	4.1252D-02
6	0	0	0	0	1	2	0.06038	18	-0.59	7.3889E-03	4.8641D-02
7	0	0	0	2	1	2	0.10688	108	-1.05	7.3388E-03	5.5980D-02
8	0	0	0	0	1	1	0.04265	9	-0.42	7.3352E-03	6.3315D-02
9	0	0	0	2	1	1	0.08915	54	-0.88	7.2855E-03	7.0600D-02
10	0	0	0	1	2	2	0.10855	108	-1.07	6.8787E-03	7.7479D-02
11	0	0	0	1	2	1	0.09082	54	-0.90	6.8287E-03	8.4308D-02
12	0	0	0	1	0	3	0.07644	30	-0.74	6.6174E-03	9.0925D-02
13	0	0	0	0	0	2	0.03546	6	-0.34	6.4586E-03	9.7384D-02
14	0	0	0	2	0	2	0.08195	36	-0.80	6.4147E-03	1.0380D-01
15	0	0	0	0	0	1	0.01773	3	-0.17	6.4116E-03	1.1021D-01
16	0	0	0	2	0	1	0.06422	18	-0.63	6.3681E-03	1.1658D-01
17	0	0	0	0	1	3	0.07811	30	-0.76	6.2025E-03	1.2278D-01
18	0	0	0	2	1	3	0.12460	180	-1.22	6.1604E-03	1.2894D-01
19	0	0	0	1	1	0	0.04817	9	-0.48	5.9255E-03	1.3487D-01
20	0	0	0	1	2	3	0.12628	180	-1.24	5.7742E-03	1.4064D-01
21	0	0	0	1	1	4	0.11909	135	-1.16	5.7196E-03	1.4636D-01
22	0	0	0	0	2	2	0.08530	36	-0.84	5.6356E-03	1.5200D-01
23	0	0	0	2	2	2	0.13180	216	-1.30	5.5973E-03	1.5759D-01
24	0	0	0	0	2	1	0.06757	18	-0.67	5.5946E-03	1.6319D-01
25	0	0	0	2	2	1	0.11407	108	-1.13	5.5567E-03	1.6874D-01
26	0	0	0	0	0	3	0.05319	10	-0.51	5.4215E-03	1.7417D-01
27	0	0	0	2	0	3	0.09968	60	-0.97	5.3847E-03	1.7955D-01
28	0	0	0	1	0	0	0.02325	3	-0.23	5.1794E-03	1.8473D-01
29	0	0	0	1	0	4	0.09417	45	-0.91	4.9994E-03	1.8973D-01
30	0	0	0	3	1	2	0.13012	180	-1.28	4.9764E-03	1.9471D-01
31	0	0	0	3	1	1	0.11239	90	-1.11	4.9403E-03	1.9965D-01
32	0	0	0	0	1	0	0.02492	3	-0.25	4.8546E-03	2.0450D-01
33	0	0	0	2	1	0	0.07142	18	-0.71	4.8217E-03	2.0932D-01
34	0	0	0	0	2	3	0.10303	60	-1.01	4.7307E-03	2.1405D-01
35	0	0	0	2	2	3	0.14953	360	-1.47	4.6986E-03	2.1875D-01
36	0	0	0	0	1	4	0.09584	45	-0.93	4.6859E-03	2.2344D-01
37	0	0	0	2	1	4	0.14233	270	-1.39	4.6541E-03	2.2809D-01
38	0	0	0	1	2	0	0.07309	18	-0.73	4.5194E-03	2.3261D-01
39	0	0	0	1	3	2	0.13347	180	-1.32	4.3720E-03	2.3698D-01
40	0	0	0	1	2	4	0.14401	270	-1.41	4.3623E-03	2.4135D-01

Continued

NO.	V1	V2	V3	V4	V5	V6	E(EV)	DH	SHIFT	POPULATION	CUSUM
41	0	0	0	3	0	2	0.10520	60	-1.03	4.3498E-03	2.4570D-01
42	0	0	0	1	3	1	0.11574	90	-1.15	4.3402E-03	2.5004D-01
43	0	0	0	3	0	1	0.08747	30	-0.86	4.3182E-03	2.5435D-01
44	0	0	0	0	0	0	0.0	1	0.0	4.2434E-03	2.5860D-01
45	0	0	0	2	0	0	0.04649	6	-0.46	4.2146E-03	2.6281D-01
46	0	0	0	3	1	3	0.14785	300	-1.45	4.1774E-03	2.6699D-01
47	0	0	0	0	0	4	0.07092	15	-0.68	4.0959E-03	2.7108D-01
48	0	0	0	2	0	4	0.11741	90	-1.14	4.0681E-03	2.7515D-01
49	0	0	0	1	1	5	0.13682	189	-1.33	4.0330E-03	2.7919D-01
50	0	0	0	3	2	2	0.15504	360	-1.53	3.7956E-03	2.8298D-01
51	0	0	0	3	2	1	0.13731	180	-1.36	3.7680E-03	2.8675D-01
52	0	0	0	0	2	0	0.04984	6	-0.50	3.7026E-03	2.9045D-01
53	0	0	0	2	2	0	0.09634	36	-0.96	3.6775E-03	2.9413D-01
54	0	0	0	1	3	3	0.15120	300	-1.49	3.6700E-03	2.9780D-01
55	0	0	0	3	0	3	0.12293	100	-1.20	3.6514E-03	3.0145D-01
56	0	0	0	0	3	2	0.11022	60	-1.09	3.5819E-03	3.0503D-01
57	0	0	0	0	2	4	0.12076	90	-1.18	3.5740E-03	3.0861D-01
58	0	0	0	2	3	2	0.15672	360	-1.55	3.5576E-03	3.1216D-01
59	0	0	0	0	3	1	0.09249	30	-0.92	3.5559E-03	3.1572D-01
60	0	0	0	2	2	4	0.16726	540	-1.64	3.5497E-03	3.1927D-01
61	0	0	0	2	3	1	0.13899	180	-1.38	3.5317E-03	3.2280D-01
62	0	0	0	1	0	5	0.11190	63	-1.08	3.5252E-03	3.2633D-01
63	0	0	0	0	1	5	0.11357	63	-1.10	3.3042E-03	3.2963D-01
64	0	0	0	2	1	5	0.16006	378	-1.56	3.2817E-03	3.3291D-01
65	0	0	0	3	1	0	0.09466	30	-0.94	3.2696E-03	3.3618D-01
66	0	0	0	3	2	3	0.17277	600	-1.70	3.1861E-03	3.3937D-01
67	0	0	0	3	1	4	0.16558	450	-1.62	3.1560E-03	3.4252D-01
68	0	0	0	1	2	5	0.16174	378	-1.58	3.0760E-03	3.4560D-01
69	0	0	0	4	1	2	0.15337	270	-1.51	3.0371E-03	3.4864D-01
70	0	0	0	4	1	1	0.13564	135	-1.34	3.0150E-03	3.5165D-01
71	0	0	0	0	3	3	0.12795	100	-1.26	3.0068E-03	3.5466D-01
72	0	0	0	2	3	3	0.17445	600	-1.72	2.9864E-03	3.5765D-01
73	0	0	0	0	0	5	0.08865	21	-0.85	2.8881E-03	3.6053D-01
74	0	0	0	1	3	0	0.09801	30	-0.98	2.8725E-03	3.6341D-01
75	0	0	0	2	0	5	0.13514	126	-1.31	2.8685E-03	3.6627D-01
76	0	0	0	3	0	0	0.06974	10	-0.69	2.8579E-03	3.6913D-01
77	0	0	0	1	3	4	0.16893	450	-1.66	2.7726E-03	3.7191D-01
78	0	0	0	3	0	4	0.14066	150	-1.37	2.7586E-03	3.7466D-01
79	0	0	0	1	1	6	0.15455	252	-1.50	2.7083E-03	3.7737D-01
80	0	0	0	4	0	2	0.12845	90	-1.26	2.6547E-03	3.8003D-01

Continued

NO.	V1	V2	V3	V4	V5	V6	E(EV)	DH	SHIFT	POPULATION	CUSUM
81	0	0	0	4	0	1	0.11072	45	-1.09	2.6354E-03	3.8266D-01
82	0	0	0	4	1	3	0.17110	450	-1.68	2.5494E-03	3.8521D-01
83	0	0	0	0	2	5	0.13849	126	-1.35	2.5201E-03	3.8773D-01
84	0	0	0	2	2	5	0.18499	756	-1.81	2.5030E-03	3.9023D-01
85	0	0	0	1	4	2	0.15839	270	-1.57	2.5009E-03	3.9274D-01
86	0	0	0	3	2	0	0.11958	60	-1.19	2.4937E-03	3.9523D-01
87	0	0	0	1	4	1	0.14066	135	-1.40	2.4827E-03	3.9771D-01
88	0	0	0	3	3	2	0.17996	600	-1.78	2.4124E-03	4.0012D-01
89	0	0	0	3	2	4	0.19050	900	-1.87	2.4071E-03	4.0253D-01
90	0	0	0	3	3	1	0.16223	300	-1.61	2.3949E-03	4.0493D-01
91	0	0	0	1	0	6	0.12963	84	-1.25	2.3673E-03	4.0729D-01
92	0	0	0	0	3	0	0.07476	10	-0.75	2.3534E-03	4.0965D-01
93	0	0	0	2	3	0	0.12126	60	-1.21	2.3374E-03	4.1198D-01
94	0	0	0	4	2	2	0.17829	540	-1.76	2.3164E-03	4.1430D-01
95	0	0	0	4	2	1	0.16056	270	-1.59	2.2996E-03	4.1660D-01
96	0	0	0	0	3	4	0.14568	150	-1.43	2.2716E-03	4.1887D-01
97	0	0	0	2	3	4	0.19218	900	-1.89	2.2562E-03	4.2113D-01
98	0	0	0	4	0	3	0.14618	150	-1.43	2.2284E-03	4.2336D-01
99	0	0	0	3	1	5	0.18331	630	-1.79	2.2254E-03	4.2558D-01
100	0	0	0	0	1	6	0.13130	84	-1.27	2.2189E-03	4.2780D-01
101	0	0	0	2	1	6	0.17779	504	-1.73	2.2038E-03	4.3000D-01
102	0	0	0	1	4	3	0.17612	450	-1.74	2.0993E-03	4.3210D-01
103	0	0	0	1	2	6	0.17947	504	-1.75	2.0657E-03	4.3417D-01
104	0	0	0	0	4	2	0.13514	90	-1.34	2.0489E-03	4.3622D-01
105	0	0	0	2	4	2	0.18164	540	-1.80	2.0350E-03	4.3825D-01
106	0	0	0	0	4	1	0.11741	45	-1.17	2.0341E-03	4.4029D-01
107	0	0	0	3	3	3	0.19769	1000	-1.95	2.0250E-03	4.4231D-01
108	0	0	0	2	4	1	0.16391	270	-1.63	2.0202E-03	4.4433D-01
109	0	0	0	4	1	0	0.11791	45	-1.17	1.9954E-03	4.4633D-01
110	0	0	0	1	3	5	0.18666	630	-1.83	1.9551E-03	4.4828D-01
111	0	0	0	3	0	5	0.15839	210	-1.54	1.9451E-03	4.5023D-01
112	0	0	0	4	2	3	0.19602	900	-1.93	1.9445E-03	4.5217D-01
113	0	0	0	0	0	6	0.10638	28	-1.02	1.9395E-03	4.5411D-01
114	0	0	0	2	0	6	0.15287	168	-1.48	1.9263E-03	4.5604D-01
115	0	0	0	4	1	4	0.18883	675	-1.85	1.9261E-03	4.5797D-01
116	0	0	0	1	1	7	0.17228	324	-1.67	1.7538E-03	4.5972D-01
117	0	0	0	4	0	0	0.09299	15	-0.92	1.7441E-03	4.6146D-01
118	0	0	0	5	1	2	0.17662	378	-1.74	1.7299E-03	4.6319D-01
119	0	0	0	0	4	3	0.15287	150	-1.51	1.7199E-03	4.6491D-01
120	0	0	0	5	1	1	0.15889	189	-1.57	1.7174E-03	4.6663D-01

Continued

NO.	V1	V2	V3	V4	V5	V6	E(EV)	DH	SHIFT	POPULATION	CUSUM
121	0	0	0	2	4	3	0.19937	900	-1.97	1.7083E-03	4.6834D-01
122	0	0	0	3	2	5	0.20823	1260	-2.04	1.6973E-03	4.7004D-01
123	0	0	0	0	2	6	0.15622	168	-1.52	1.6924E-03	4.7173D-01
124	0	0	0	4	0	4	0.16391	225	-1.60	1.6835E-03	4.7341D-01
125	0	0	0	2	2	6	0.20272	1008	-1.98	1.6809E-03	4.7509D-01
126	0	0	0	1	4	0	0.12293	45	-1.23	1.6431E-03	4.7674D-01
127	0	0	0	0	3	5	0.16341	210	-1.60	1.6017E-03	4.7834D-01
128	0	0	0	2	3	5	0.20991	1260	-2.06	1.5909E-03	4.7993D-01
129	0	0	0	1	4	4	0.19385	675	-1.91	1.5860E-03	4.8151D-01
130	0	0	0	3	3	0	0.14450	100	-1.44	1.5850E-03	4.8310D-01
131	0	0	0	1	0	7	0.14736	108	-1.42	1.5330E-03	4.8463D-01
132	0	0	0	3	3	4	0.21542	1500	-2.12	1.5299E-03	4.8616D-01
133	0	0	0	4	2	0	0.14283	90	-1.42	1.5219E-03	4.8768D-01
134	0	0	0	5	0	2	0.15170	126	-1.49	1.5121E-03	4.8920D-01
135	0	0	0	5	0	1	0.13397	63	-1.32	1.5011E-03	4.9070D-01
136	0	0	0	3	1	6	0.20104	840	-1.96	1.4944E-03	4.9219D-01
137	0	0	0	4	3	2	0.20321	900	-2.01	1.4723E-03	4.9366D-01
138	0	0	0	4	2	4	0.21375	1350	-2.10	1.4690E-03	4.9513D-01
139	0	0	0	4	3	1	0.18548	450	-1.84	1.4616E-03	4.9659D-01
140	0	0	0	5	1	3	0.19435	630	-1.91	1.4522E-03	4.9805D-01
141	0	0	0	0	1	7	0.14903	108	-1.44	1.4369E-03	4.9948D-01
142	0	0	0	2	1	7	0.19552	648	-1.90	1.4271E-03	5.0091D-01
143	0	1	0	1	1	2	0.14990	108	-3.52	1.3894E-03	5.0230D-01
144	0	0	0	3	4	2	0.20489	900	-2.03	1.3800E-03	5.0368D-01
145	0	1	0	1	1	1	0.13217	54	-3.35	1.3793E-03	5.0506D-01
146	0	0	0	3	4	1	0.18716	450	-1.86	1.3699E-03	5.0643D-01
147	0	0	0	4	1	5	0.20656	945	-2.02	1.3581E-03	5.0779D-01
148	0	0	0	0	4	0	0.09968	15	-1.00	1.3462E-03	5.0913D-01
149	0	0	0	1	2	7	0.19720	648	-1.92	1.3376E-03	5.1047D-01
150	0	0	0	2	4	0	0.14618	90	-1.46	1.3370E-03	5.1181D-01
151	0	0	0	1	5	2	0.18331	378	-1.82	1.3352E-03	5.1314D-01
152	0	0	1	1	1	2	0.16145	162	-2.62	1.3329E-03	5.1448D-01
153	0	0	0	1	5	1	0.16558	189	-1.65	1.3255E-03	5.1580D-01
154	0	0	1	1	1	1	0.14372	81	-2.45	1.3232E-03	5.1713D-01
155	0	0	0	5	2	2	0.20154	756	-1.99	1.3194E-03	5.1844D-01
156	0	0	0	1	3	6	0.20439	840	-2.00	1.3129E-03	5.1976D-01
157	0	0	0	5	2	1	0.18381	378	-1.82	1.3098E-03	5.2107D-01
158	0	0	0	3	0	6	0.17612	280	-1.71	1.3063E-03	5.2237D-01
159	0	0	0	0	4	4	0.17060	225	-1.68	1.2994E-03	5.2367D-01
160	0	0	0	2	4	4	0.21710	1350	-2.14	1.2906E-03	5.2496D-01

Continued

NO.	V1	V2	V3	V4	V5	V6	E(EV)	DH	SHIFT	POPULATION	CUSUM
161	0	0	0	5	0	3	0.16943	210	-1.66	1.2693E-03	5.2623D-01
162	0	0	0	0	0	7	0.12411	36	-1.19	1.2560E-03	5.2749D-01
163	0	0	0	2	0	7	0.17060	216	-1.65	1.2474E-03	5.2874D-01
164	0	0	0	4	3	3	0.22094	1500	-2.18	1.2359E-03	5.2997D-01
165	0	1	0	1	0	2	0.12498	36	-3.27	1.2145E-03	5.3119D-01
166	0	1	0	1	0	1	0.10725	18	-3.10	1.2057E-03	5.3239D-01
167	0	0	0	4	0	5	0.18164	315	-1.77	1.1871E-03	5.3358D-01
168	0	1	0	1	1	3	0.16763	180	-3.69	1.1663E-03	5.3475D-01
169	0	0	1	1	0	2	0.13653	54	-2.37	1.1651E-03	5.3591D-01
170	0	0	0	3	4	3	0.22262	1500	-2.20	1.1584E-03	5.3707D-01
171	0	0	1	1	0	1	0.11880	27	-2.20	1.1566E-03	5.3823D-01
172	0	0	0	3	2	6	0.22596	1680	-2.21	1.1398E-03	5.3937D-01
173	0	1	0	0	1	2	0.12665	36	-3.29	1.1383E-03	5.4050D-01
174	0	0	0	5	1	0	0.14116	63	-1.40	1.1366E-03	5.4164D-01
175	0	1	0	2	1	2	0.17314	216	-3.75	1.1306E-03	5.4277D-01
176	0	1	0	0	1	1	0.10892	18	-3.12	1.1301E-03	5.4390D-01
177	0	1	0	2	1	1	0.15542	108	-3.58	1.1224E-03	5.4502D-01
178	0	0	0	1	5	3	0.20104	630	-1.99	1.1208E-03	5.4614D-01
179	0	0	1	1	1	3	0.17918	270	-2.79	1.1189E-03	5.4726D-01
180	0	0	0	1	4	5	0.21158	945	-2.08	1.1183E-03	5.4838D-01
181	0	0	0	5	2	3	0.21927	1260	-2.16	1.1076E-03	5.4949D-01
182	0	0	0	1	1	8	0.19001	405	-1.84	1.1042E-03	5.5059D-01
183	0	0	0	5	1	4	0.21208	945	-2.08	1.0971E-03	5.5169D-01
184	0	0	0	0	2	7	0.17395	216	-1.69	1.0959E-03	5.5279D-01
185	0	0	0	0	5	2	0.16006	126	-1.59	1.0939E-03	5.5388D-01
186	0	0	1	0	1	2	0.13821	54	-2.39	1.0920E-03	5.5497D-01
187	0	0	0	2	2	7	0.22045	1296	-2.15	1.0885E-03	5.5606D-01
188	0	0	0	2	5	2	0.20656	756	-2.05	1.0865E-03	5.5715D-01
189	0	0	0	0	5	1	0.14233	63	-1.42	1.0860E-03	5.5823D-01
190	0	0	1	2	1	2	0.18470	324	-2.85	1.0846E-03	5.5932D-01
191	0	0	1	0	1	1	0.12048	27	-2.22	1.0841E-03	5.6040D-01
192	0	0	0	3	3	5	0.23315	2100	-2.29	1.0788E-03	5.6148D-01
193	0	0	0	2	5	1	0.18883	378	-1.88	1.0786E-03	5.6256D-01
194	0	0	1	2	1	1	0.16697	162	-2.68	1.0767E-03	5.6364D-01
195	0	0	0	0	3	6	0.18114	280	-1.77	1.0756E-03	5.6471D-01
196	0	0	0	2	3	6	0.22764	1680	-2.23	1.0683E-03	5.6578D-01
197	0	1	0	1	2	2	0.17482	216	-3.77	1.0597E-03	5.6684D-01
198	0	1	0	1	2	1	0.15709	108	-3.60	1.0520E-03	5.6789D-01
199	0	0	0	4	2	5	0.23148	1890	-2.27	1.0358E-03	5.6893D-01
200	0	1	0	1	0	3	0.14271	60	-3.44	1.0195E-03	5.6995D-01

Table 3 Calculated hot-state populations at 300K and statistical thermodynamic informations for SF_6

NO.	V1	V2	V3	V4	V5	V6	E(EV)	DH	SHIFT	POPULATION	CUSUM
1	0	0	0	0	0	0	0.0	1	0.0	3.0263E-01	3.0263D-01
2	0	0	0	0	0	1	0.04302	3	-1.00	1.7189E-01	4.7451D-01
3	0	0	0	0	1	0	0.06491	3	-0.50	7.3723E-02	5.4824D-01
4	0	0	0	0	0	2	0.08605	6	-2.00	6.5086E-02	6.1332D-01
5	0	0	0	1	0	0	0.07625	3	-1.53	4.7535E-02	6.6086D-01
6	0	0	0	0	1	1	0.10793	9	-1.50	4.1873E-02	7.0273D-01
7	0	1	0	0	0	0	0.07977	2	-2.00	2.7654E-02	7.3039D-01
8	0	0	0	1	0	1	0.11927	9	-2.53	2.6999E-02	7.5738D-01
9	0	0	0	0	0	3	0.12907	10	-3.00	2.0538E-02	7.7792D-01
10	0	0	0	0	1	2	0.15095	18	-2.50	1.5856E-02	7.9378D-01
11	0	1	0	0	0	1	0.12279	6	-3.00	1.5707E-02	8.0948D-01
12	0	0	0	0	2	0	0.12981	6	-1.00	1.1973E-02	8.2146D-01
13	0	0	0	1	1	0	0.14116	9	-2.03	1.1580E-02	8.3304D-01
14	0	0	0	1	0	2	0.16230	18	-3.53	1.0223E-02	8.4326D-01
15	0	0	1	0	0	0	0.11754	3	-3.66	9.6247E-03	8.5289D-01
16	1	0	0	0	0	0	0.09603	1	-2.90	7.3732E-03	8.6026D-01
17	0	0	0	0	2	1	0.17284	18	-2.00	6.8005E-03	8.6706D-01
18	0	1	0	0	1	0	0.14468	6	-2.50	6.7369E-03	8.7380D-01
19	0	0	0	1	1	1	0.18418	27	-3.03	6.5772E-03	8.8037D-01
20	0	1	0	0	0	2	0.16582	12	-4.00	5.9476E-03	8.8632D-01
21	0	0	0	0	0	4	0.17209	15	-4.00	5.8325E-03	8.9215D-01
22	0	0	1	0	0	1	0.16056	9	-4.66	5.4667E-03	8.9762D-01
23	0	0	0	0	1	3	0.19397	30	-3.50	5.0032E-03	9.0262D-01
24	0	0	0	2	0	0	0.15250	6	-3.06	4.9776E-03	9.0760D-01
25	0	1	0	1	0	0	0.15602	6	-3.53	4.3438E-03	9.1194D-01
26	1	0	0	0	0	1	0.13905	3	-3.90	4.1879E-03	9.1613D-01
27	0	1	0	0	1	1	0.18770	18	-3.50	3.8264E-03	9.1996D-01
28	0	0	0	1	0	3	0.20532	30	-4.53	3.2259E-03	9.2318D-01
29	0	0	0	2	0	1	0.19552	18	-4.06	2.8272E-03	9.2601D-01
30	0	0	0	0	2	2	0.21586	36	-3.00	2.5750E-03	9.2859D-01
31	0	0	0	1	1	2	0.22720	54	-4.03	2.4905E-03	9.3108D-01
32	0	1	0	1	0	1	0.19905	18	-4.53	2.4672E-03	9.3354D-01
33	0	0	1	0	1	0	0.18244	9	-4.16	2.3447E-03	9.3589D-01
34	0	0	1	0	0	2	0.20358	18	-5.66	2.0700E-03	9.3796D-01
35	0	2	0	0	0	0	0.15954	3	-4.00	1.8953E-03	9.3985D-01
36	0	0	0	1	2	0	0.20606	18	-2.53	1.8806E-03	9.4174D-01
37	0	1	0	0	0	3	0.20884	20	-5.00	1.8767E-03	9.4361D-01
38	1	0	0	0	1	0	0.16093	3	-3.40	1.7962E-03	9.4541D-01
39	0	0	0	0	3	0	0.19472	10	-1.50	1.6204E-03	9.4703D-01
40	1	0	0	0	0	2	0.18207	6	-4.90	1.5858E-03	9.4861D-01

Table 4 Coefficients of Polynominals P_5 *)

	$200cm^{-1} \leq E \leq 2000cm^{-1}$						$2000cm^{-1} \leq E \leq 5000cm^{-1}$					
Molecule	a_0	a_1	a_2	$a_3 \times 10$	$a_4 \times 10^2$	$a_5 \times 10^4$	a_0	$a_1 \times 10$	$a_2 \times 10^2$	$a_3 \times 10^4$	$a_4 \times 10^3$	$a_5 \times 10^4$
UF_6	24.97	-3.873	-1.664	3.823	-1.387	-3.324	-5.000	5.872	-4.957	4.974	5.816	-1.437
SF_6	13.17	-2.884	-0.7866	2.176	-1.090	0.7602	1.164	-6.118	-1.379	-5.589	2.438	1.329

*) $\ell nG(E) = P_n(\ell nE)$

$P_5(x) = a_0 + a_1 x + a_2 x^2 + a_3 x^3 + a_4 x^4 + a_5 x^5$

Table 5 Molecular constants used in the present simulation[a)]

Constants	UF_6	SF_6
$m \times 10^{-2}$	6.277018[b)]	9.479766[e)]
$n \times 10^{2}$	8.92061[b)]	5.58177[e)]
$p \times 10^{4}$	-0.3978[b)]	-1.61865[e)]
$q \times 10^{8}$	0[b)]	1.0391[e)]
X_{13}	-1.6[c)]	-2.9[f)]
X_{23}	-2.7[c)]	-2.0[g)]
X_{33}	-0.9[c)]	-1.83[h)]
X_{43}	-0.24[d)]	-1.53[i)]
X_{53}	-0.26[d)]	-0.5[g)]
X_{63}	-0.17[d)]	-1.0[g)]

a) All constants are in cm^{-1}
b) See Ref.(19)
c) See Ref.(2)
d) Assumed that $X_{j3} = A\nu_j$, where $A = 1.28 \times 10^{-3}$
e) See Ref.(10)
f) See Ref.(20)
g) See Ref.(22)
h) See Ref.(23)
i) See Ref.(24)

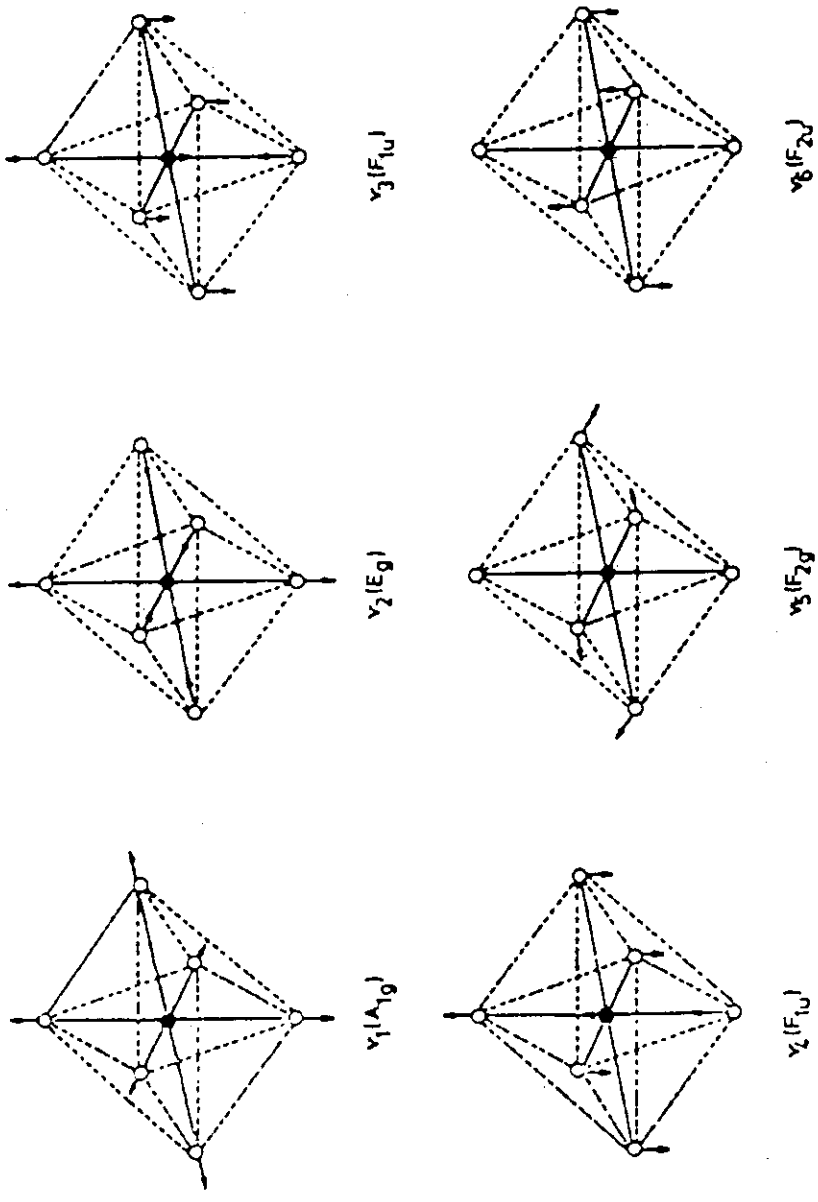

Fig.1 Fundamental modes of vibration for an XY_6 type spherical-top molecule. The symbols in parentheses represent symmetry species.

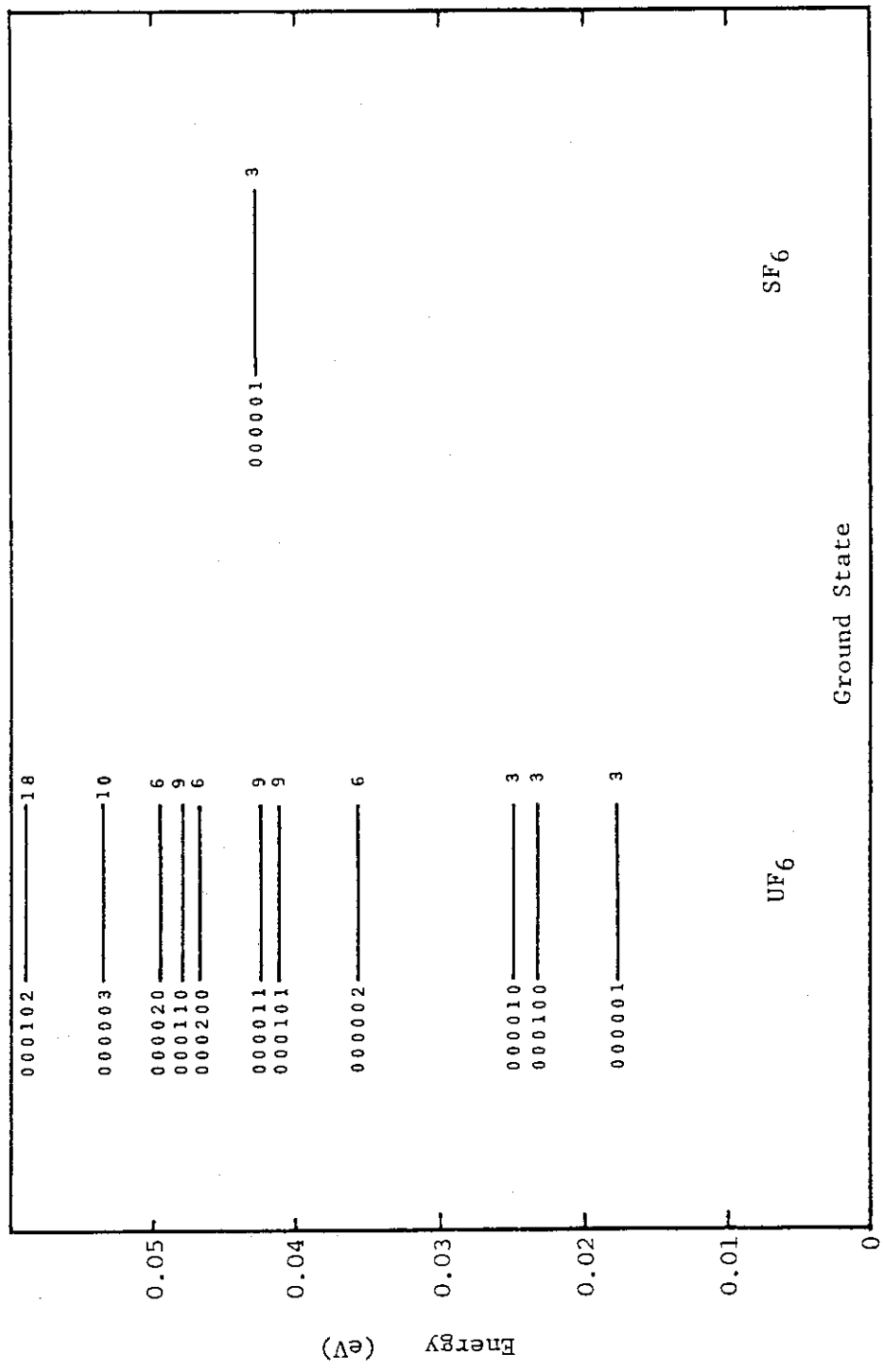

Fig.2 Vibrational energy level schemes for UF_6 and SF_6. The horizontal lines indicate the energy levels which are designated by numbers of six figures representing vibrational quantum states. The numbers at the right-hand of the levels indicate the degeneracy. The amount of energy in the ordinate is evaluated from Eq.(4).

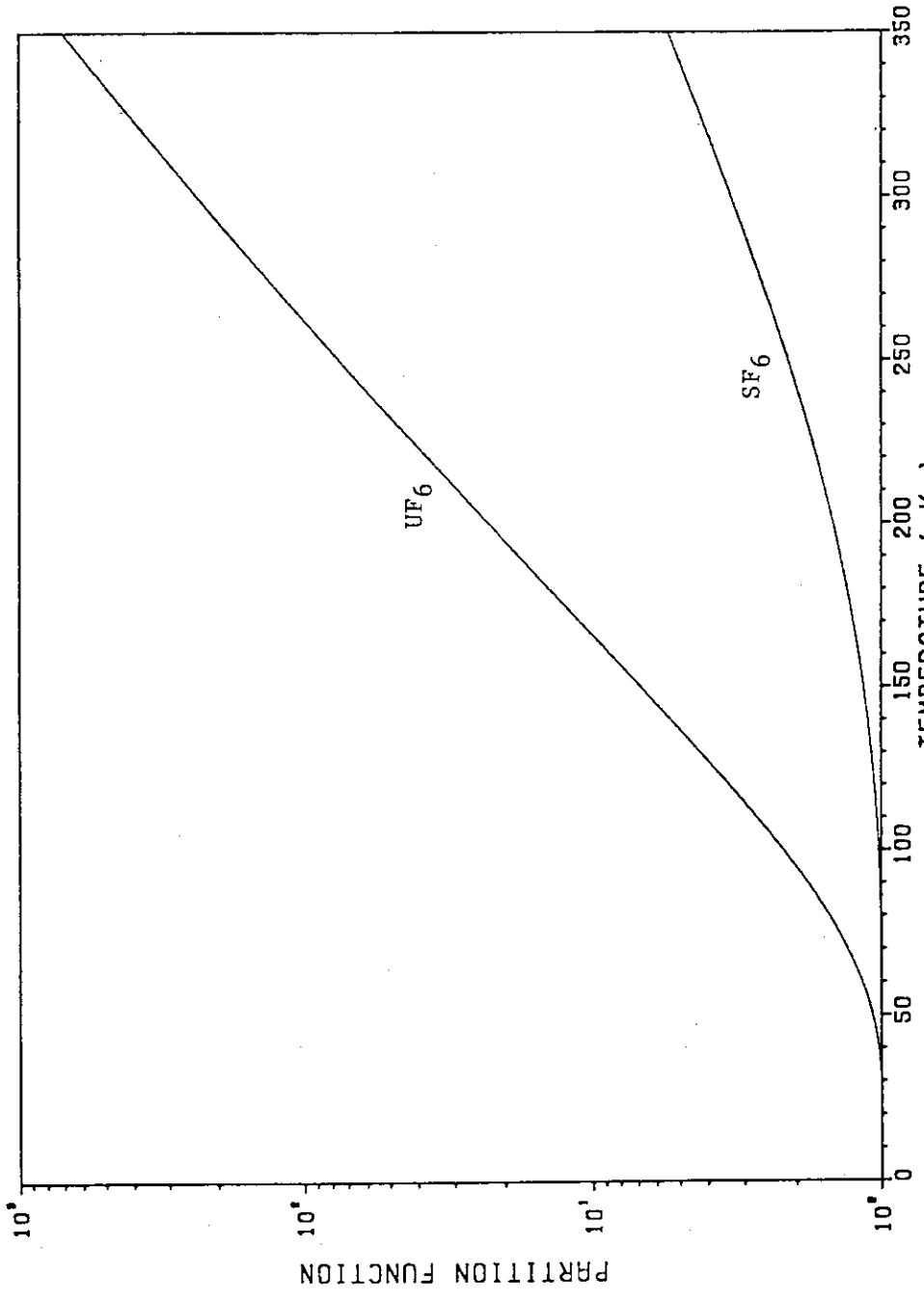

Fig.3 Vibrational partition function for UF_6 and SF_6.

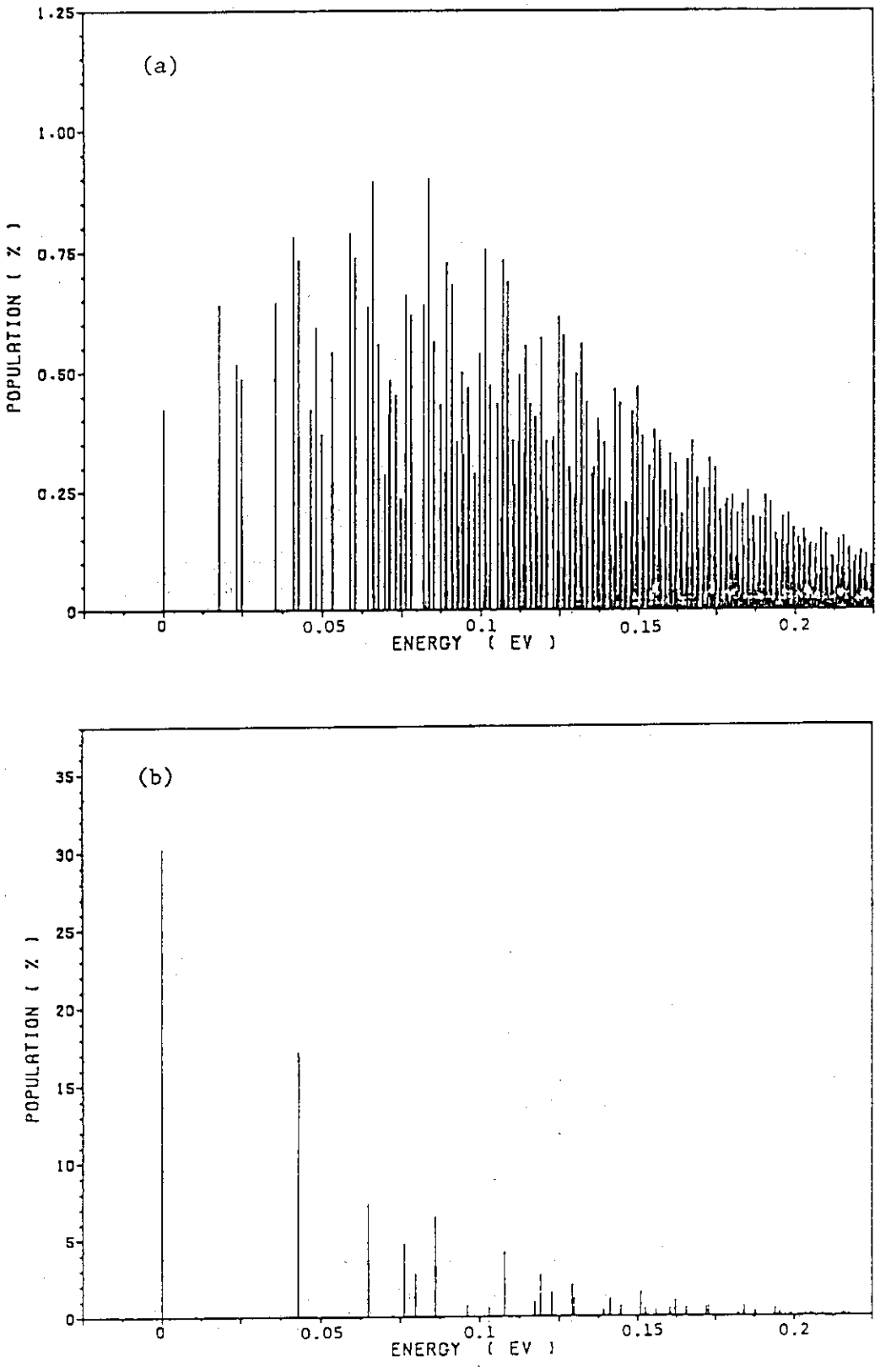

Fig.4 Population distribution for (a) UF_6 and (b) SF_6 at 300K.

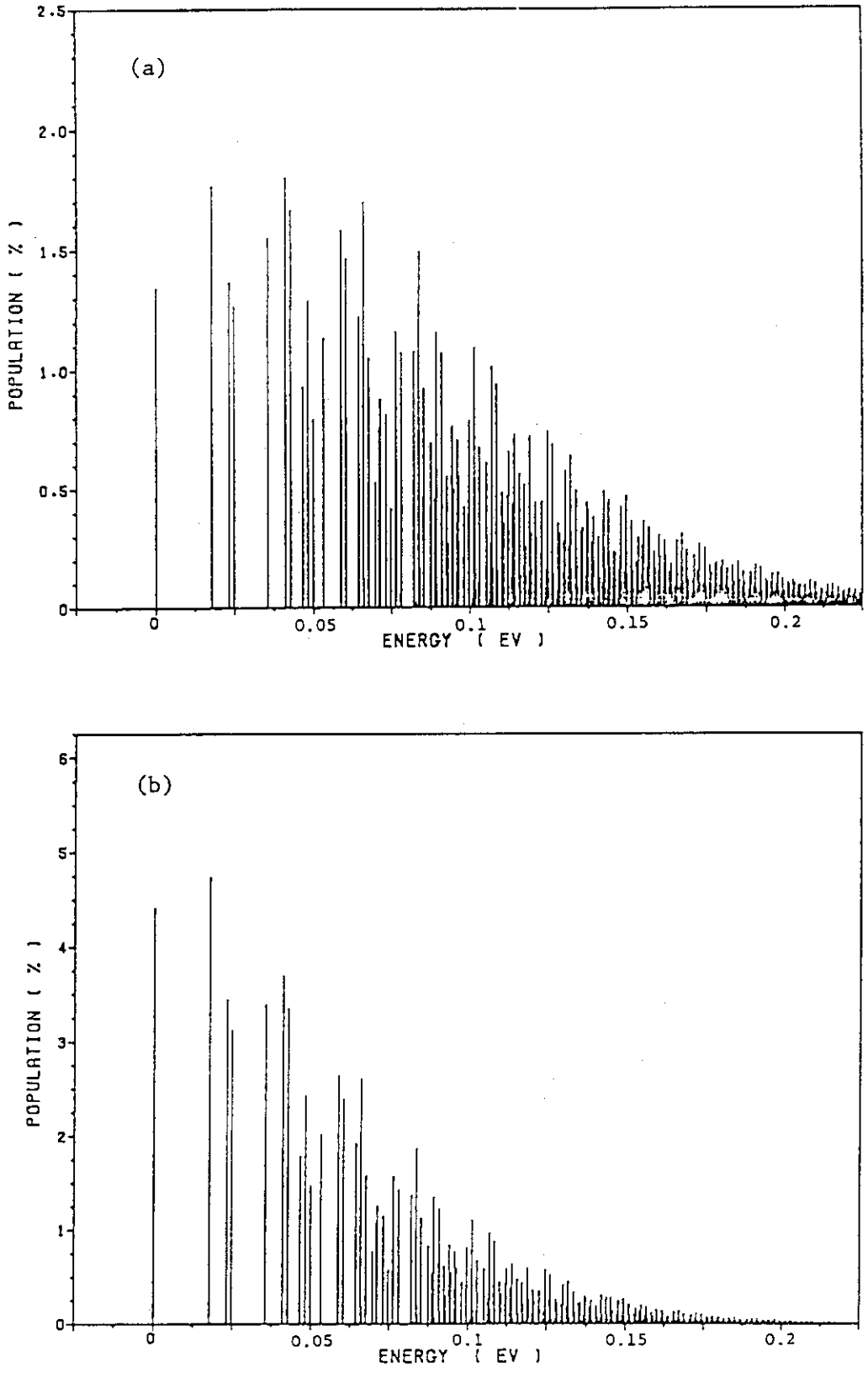

Fig.5 Population distribution for UF_6.
(a) T = 250K (b) T = 200K

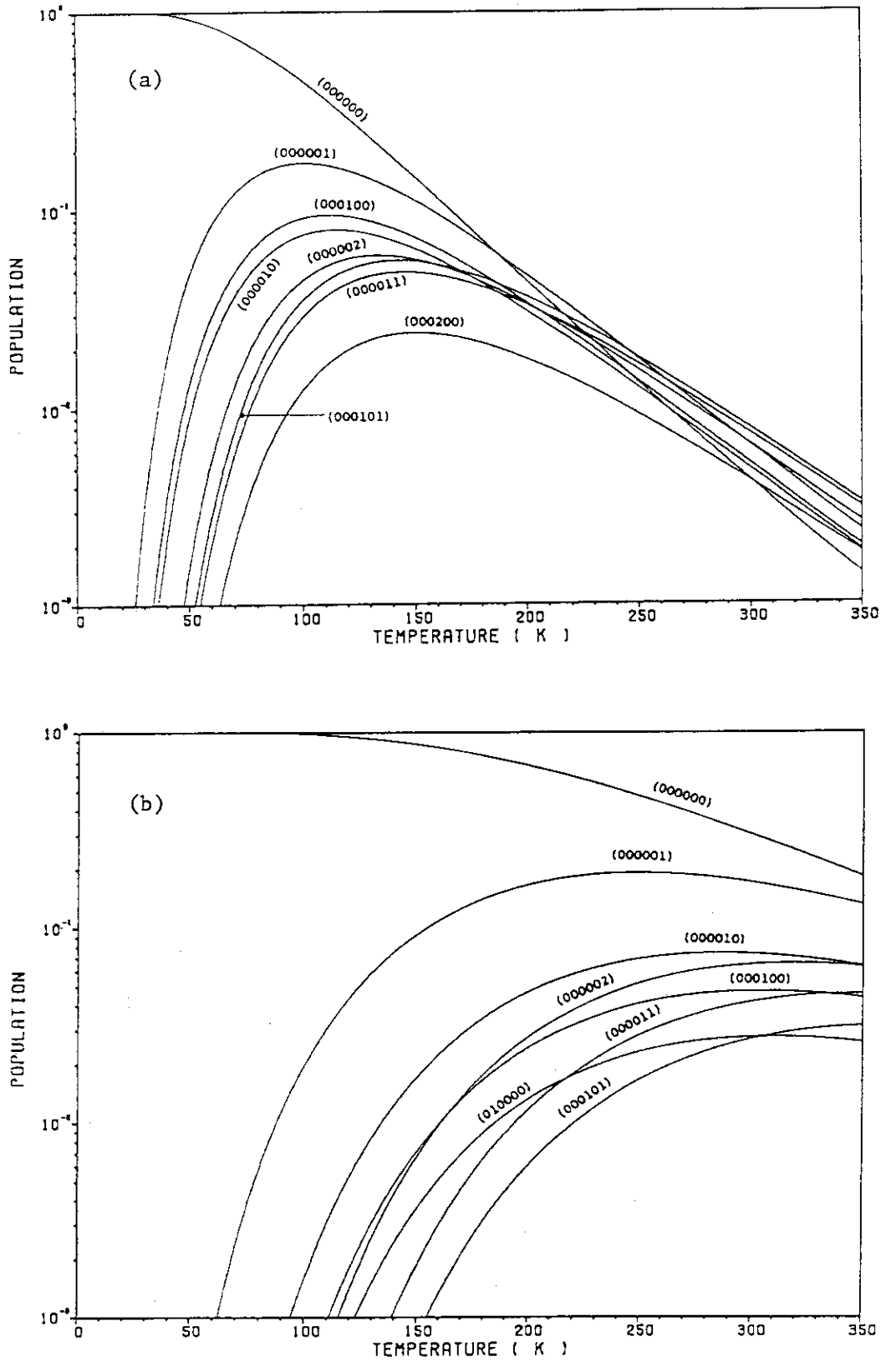

Fig.6 Fractional population of low energy vibrational levels for (a) UF_6 and (b) SF_6. It should be noted that many of actural levels are omitted since they overlap with the curves already shown here.

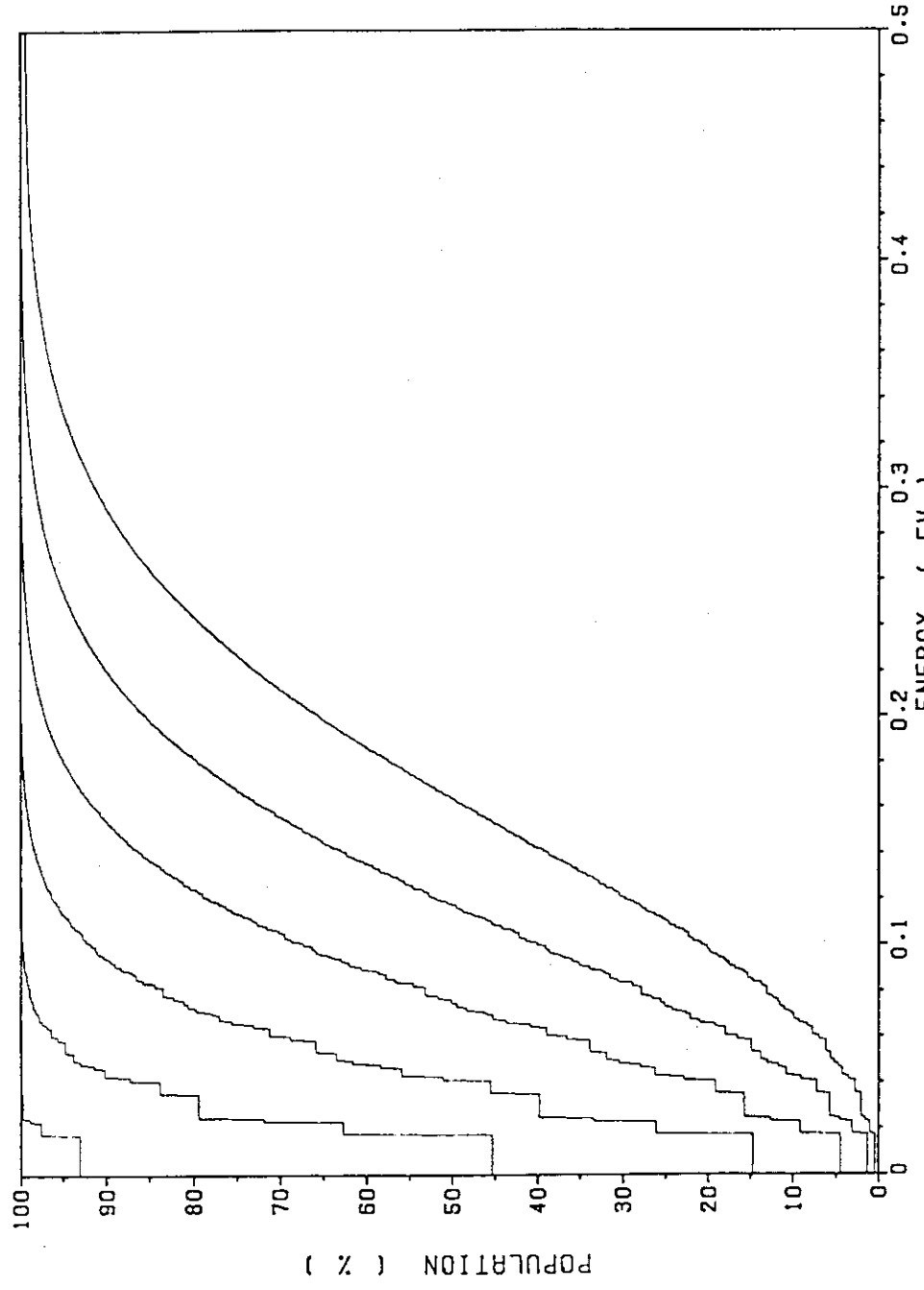

Fig.7 Cumulative population distribution for UF_6. Each curve is plotted as a function of energy for values of temperature from 50K to 300K in increments of 50K.

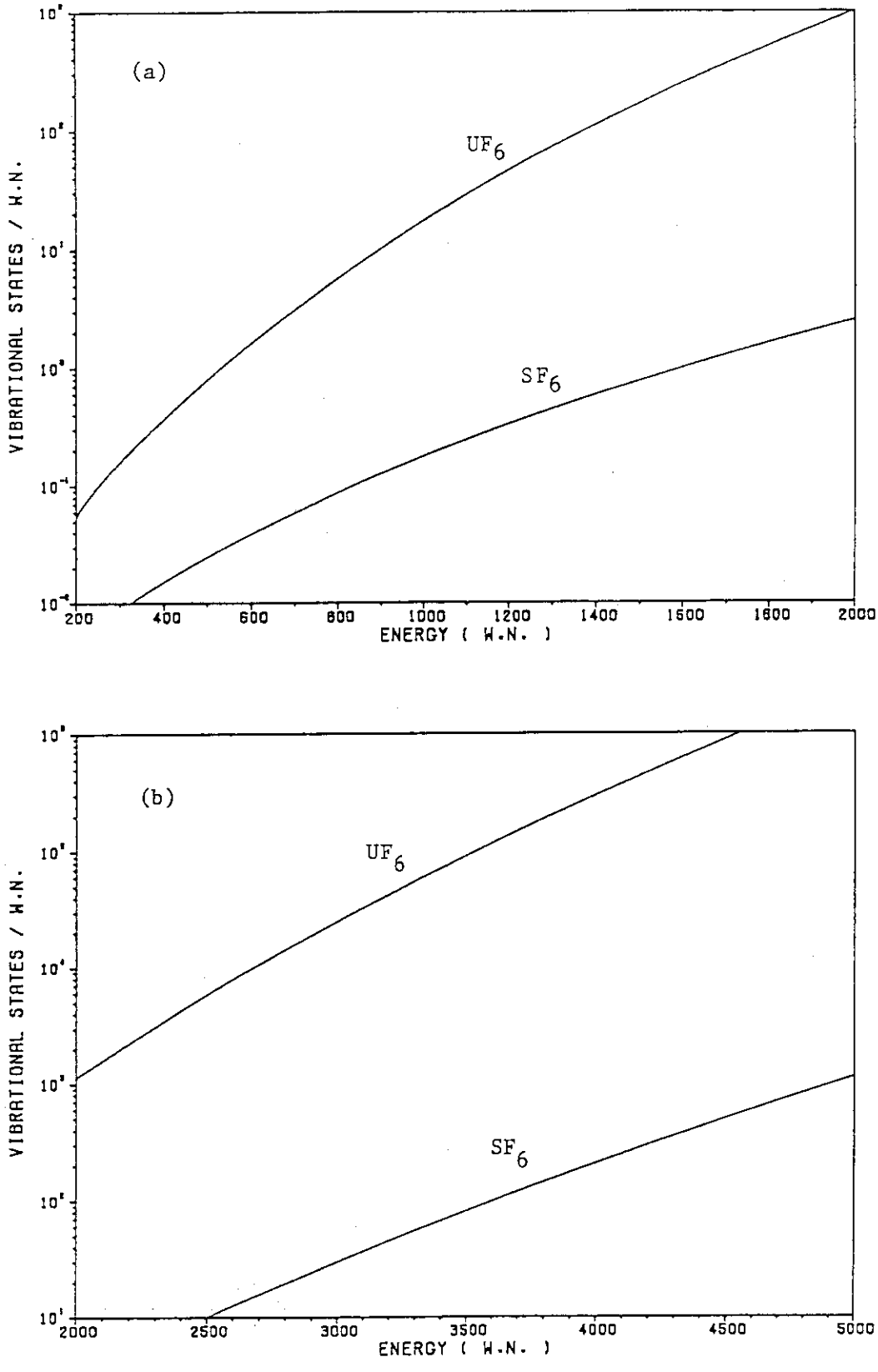

Fig.8 Density of vibrational states for UF_6 and SF_6. The ordinate g(E) is calculated from Eq.(21) where the coefficients of P_s were found in the range of energy (a) from 200 cm^{-1} to 2000 cm^{-1} and (b) from 2000 cm^{-1} to 5000 cm^{-1} individually.

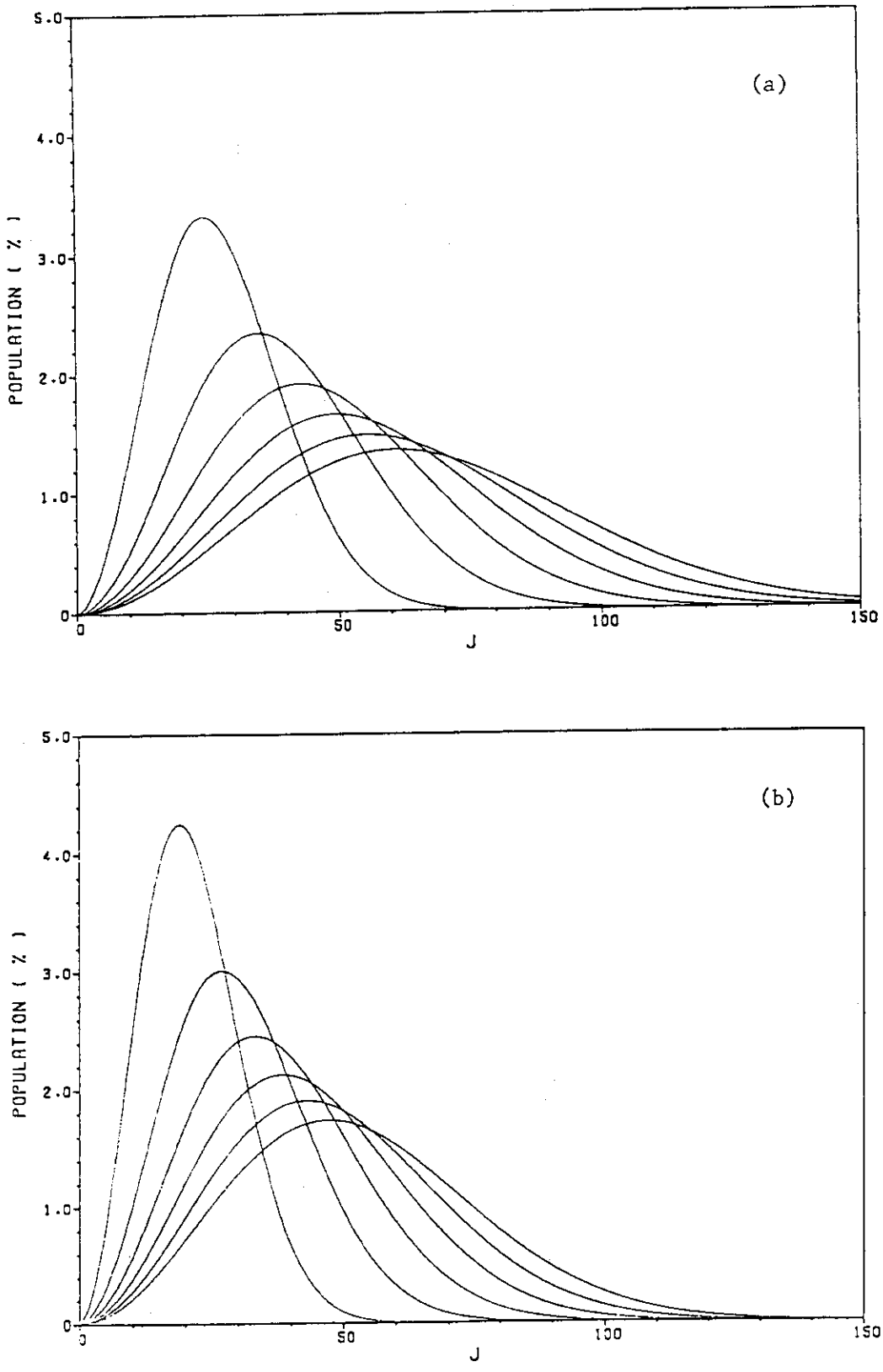

Fig.9 Rotational population for (a) UF_6 and (b) SF_6. Each curve is plotted as a function of rotational quantum number J for values of temperature from 50K to 300K in increments of 50K.

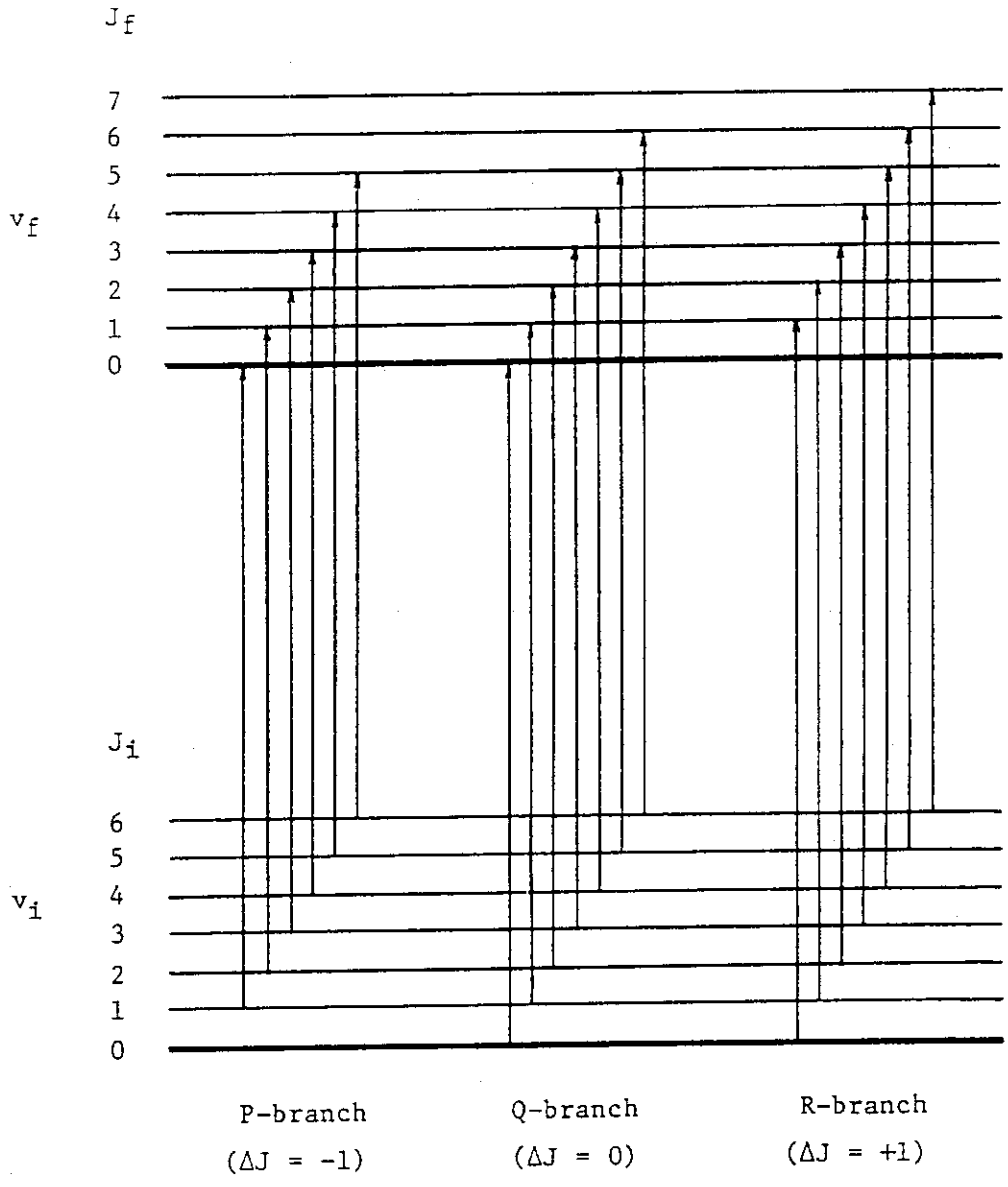

Fig.10 Allowed transitions between initial and final vibrational levels on a ro-vibrational spectrum of spherical-top molecule.

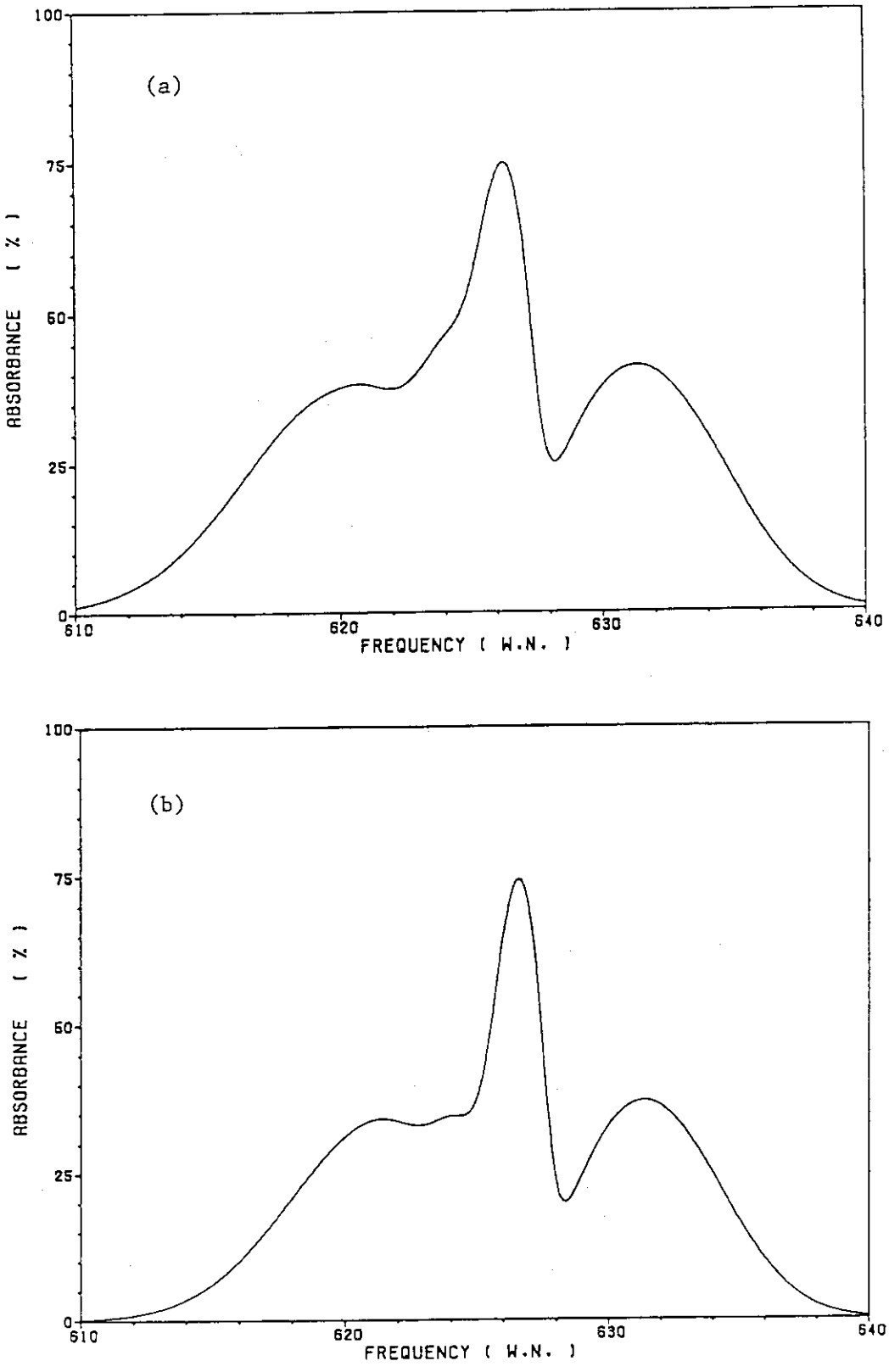

Fig.11 The UF_6 ν_3 band contours as simulated for the following conditions:
(a) T = 300K, P = 0.3 Torr, ℓ = 10 cm, FWHM = 1.0 cm^{-1}
(b) T = 250K, P = 0.19 Torr, ℓ = 10 cm, FWHM = 1.0 cm^{-1}

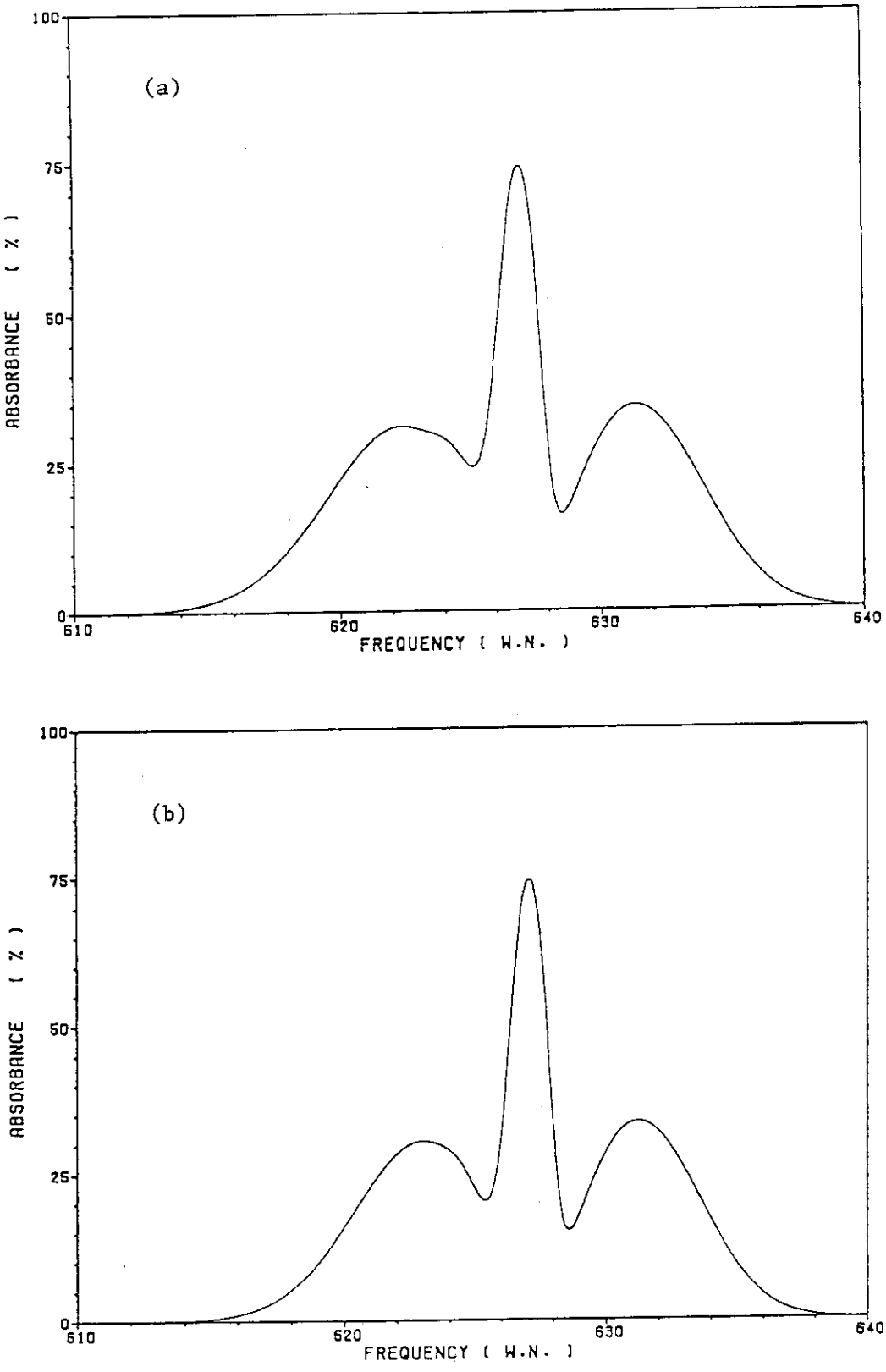

Fig.12 The UF_6 ν_3 band contours as simulated for the following conditions:
(a) T = 200K, P = 4×10^{-3} Torr, ℓ = 3 m, FWHM = 1.0 cm^{-1}
(b) T = 170K, P = 1×10^{-5} Torr, ℓ = 900 m, FWHM = 1.0 cm^{-1}

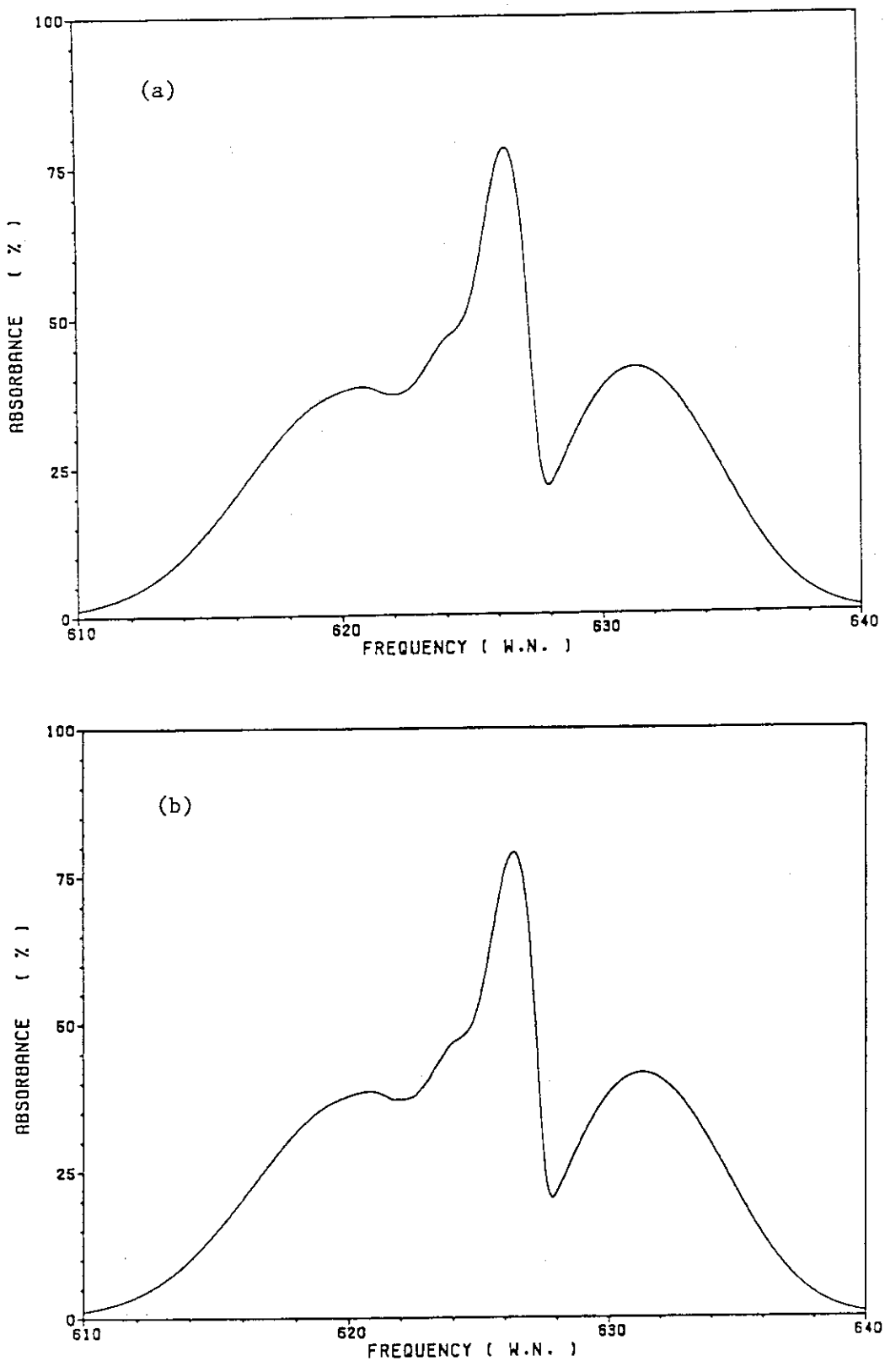

Fig.13 The UF_6 ν_3 band contours as simulated for the following conditions:
(a) T = 300K, P = 0.3 Torr, ℓ = 10 cm, FWHM = 0.5 cm^{-1}
(b) T = 300K, P = 0.3 Torr, ℓ = 10 cm, FWHM = 0.25 cm^{-1}

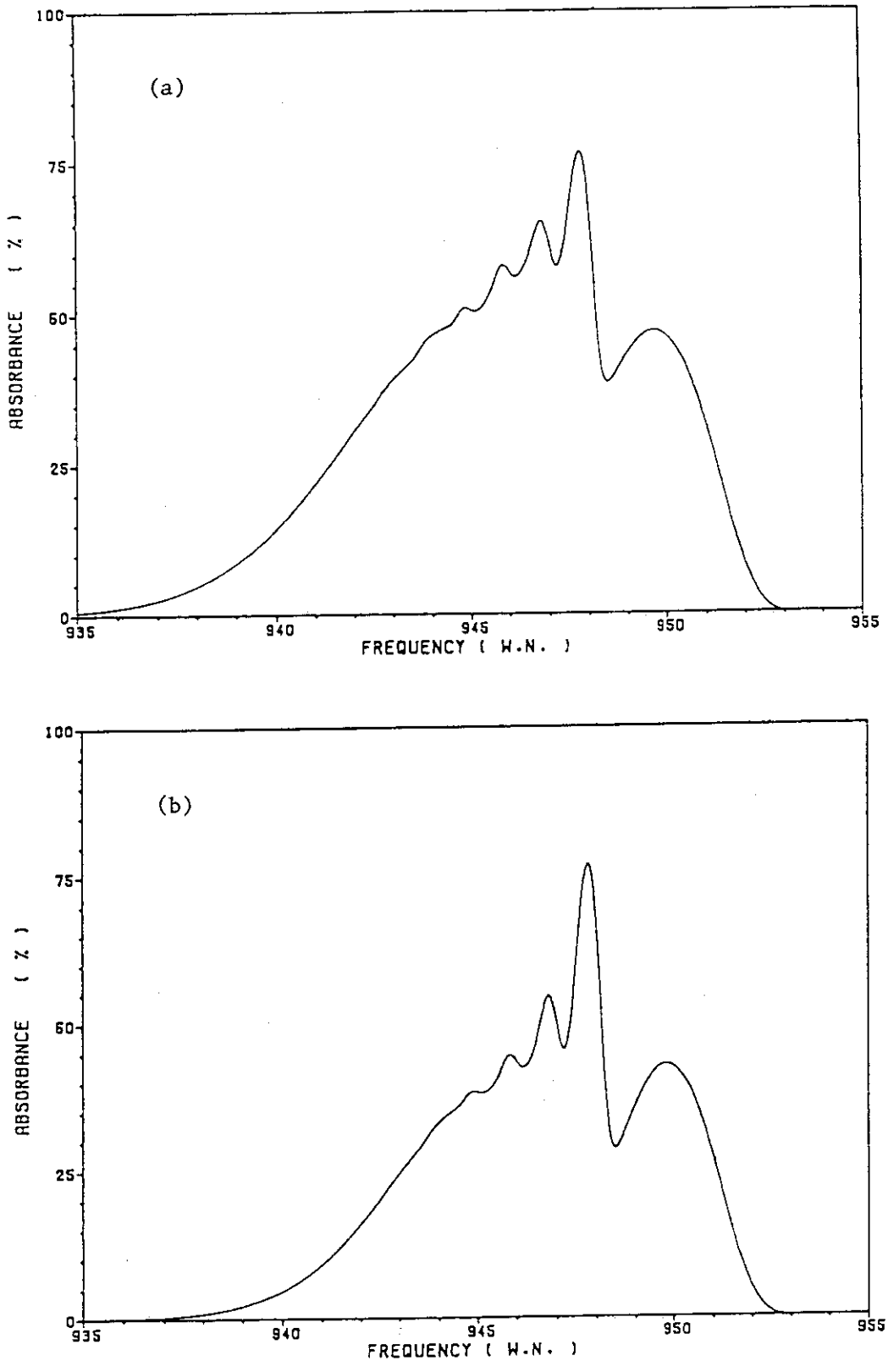

Fig.14 The SF_6 ν_3 band contours as simulated for the following conditions:
(a) T = 300K, P = 0.1 Torr, ℓ = 10 cm, FWHM = 0.5 cm^{-1}
(b) T = 250K, P = 0.058 Torr, ℓ = 10 cm, FWHM = 0.5 cm^{-1}

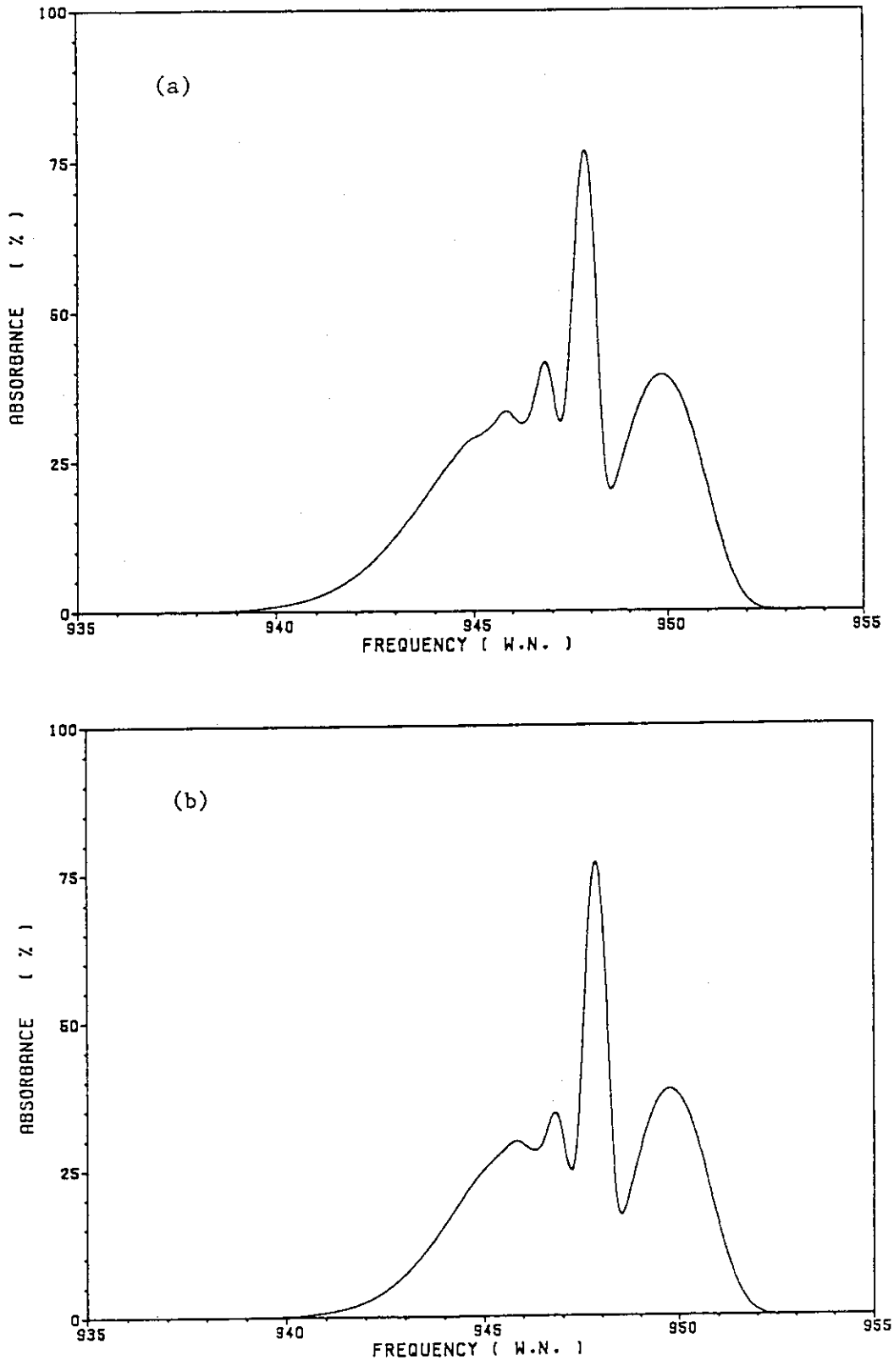

Fig.15 The SF_6 ν_3 band contours as simulated for the following conditions:
(a) T = 200K, P = 5×10^{-3} Torr, ℓ = 67 cm, FWHM = 0.5 cm^{-1}
(b) T = 170K, P = 2.2×10^{-5} Torr, ℓ = 110 m, FWHM = 0.5 cm^{-1}

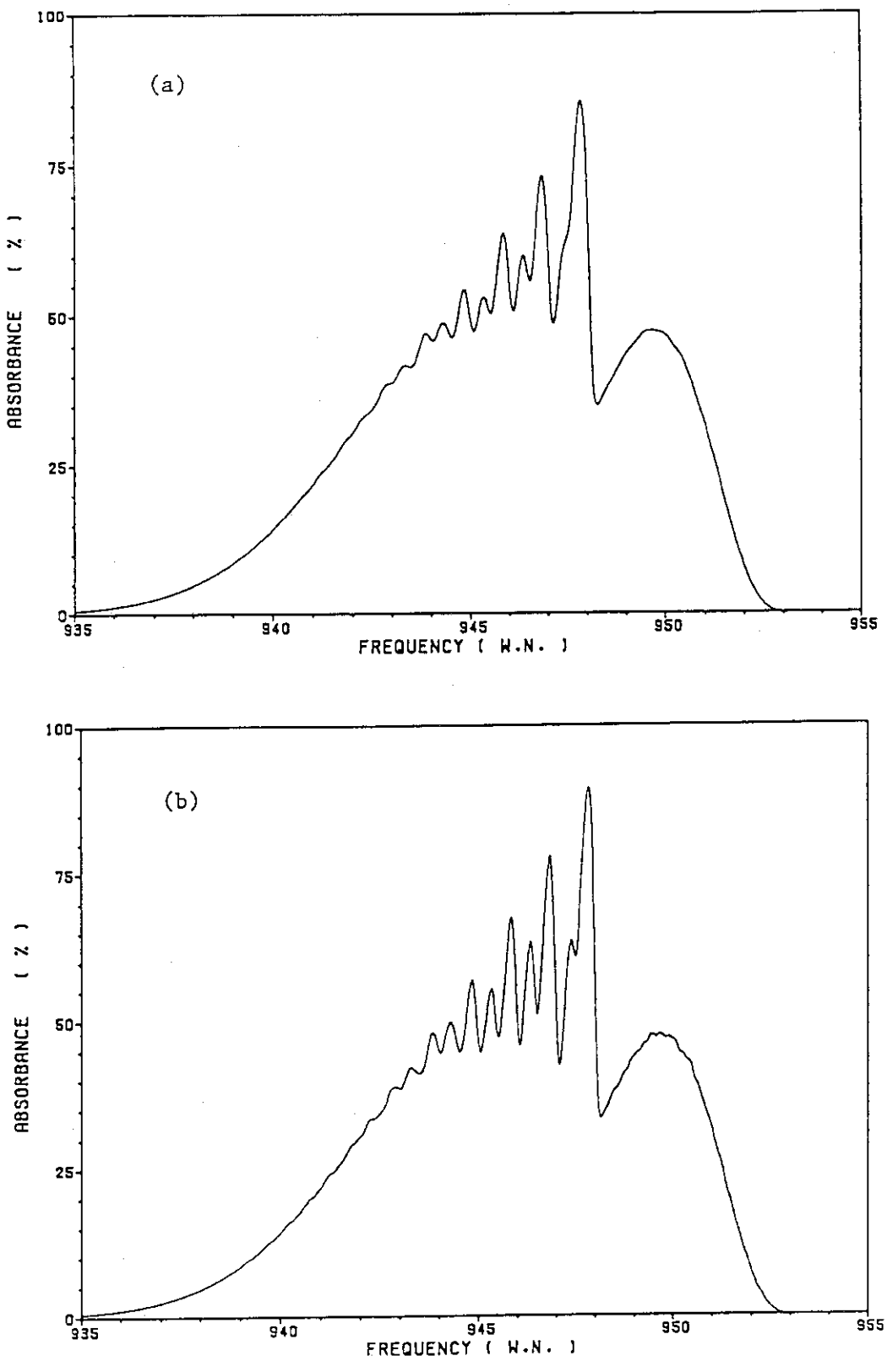

Fig.16 The SF_6 ν_3 band contours as simulated for the following conditions:
(a) T = 300K, P = 0.1 Torr, ℓ = 10 cm, FWHM = 0.25 cm^{-1}
(b) T = 300K, P = 0.1 Torr, ℓ = 10 cm, FWHM = 0.15 cm^{-1}

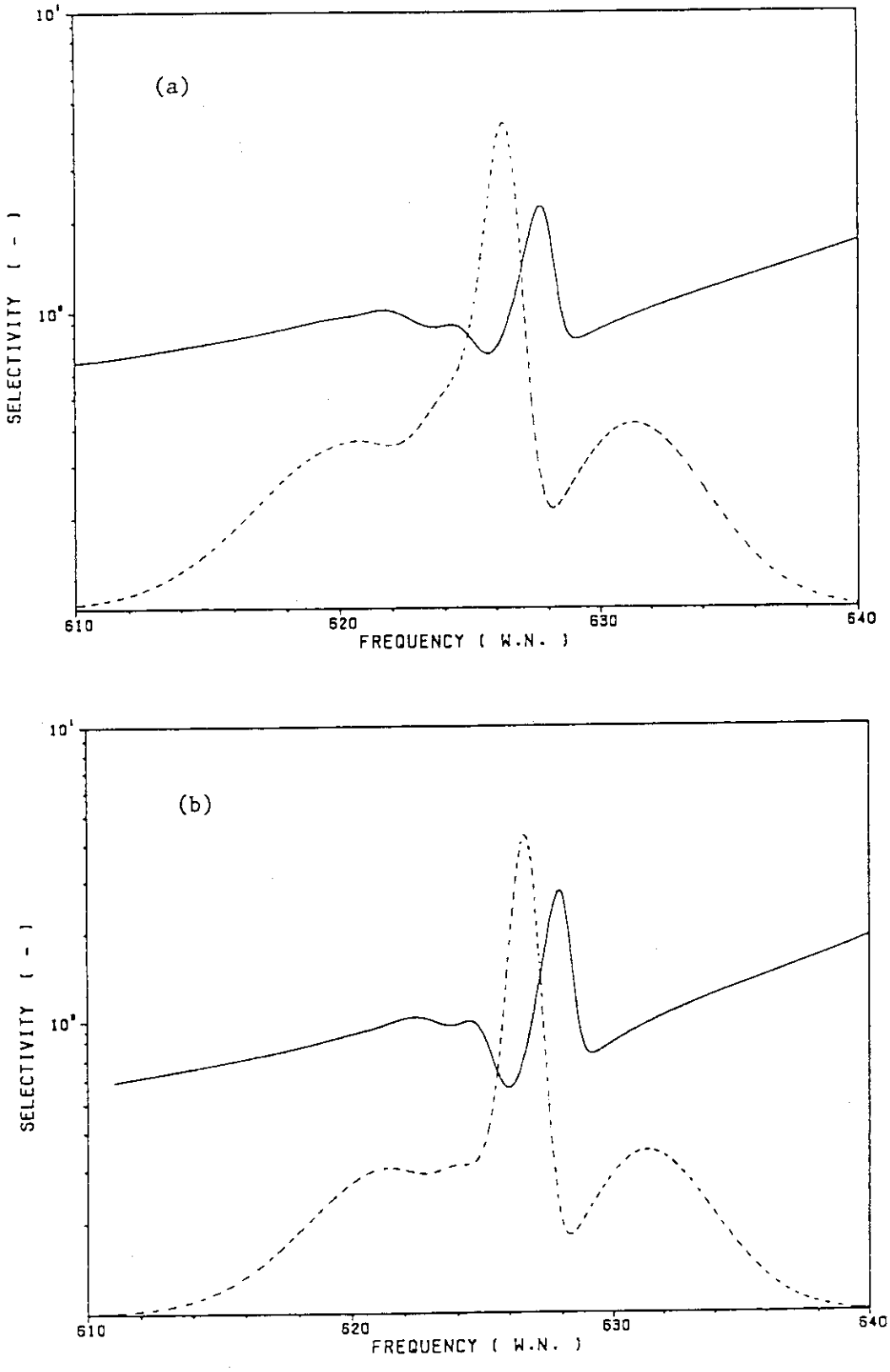

Fig.17 Isotopic selectivity as a function of absorption frequency at temperatures of (a) 300K, and (b) 250K (solid lines) compared with the ν_3 band contours (dashed lines).

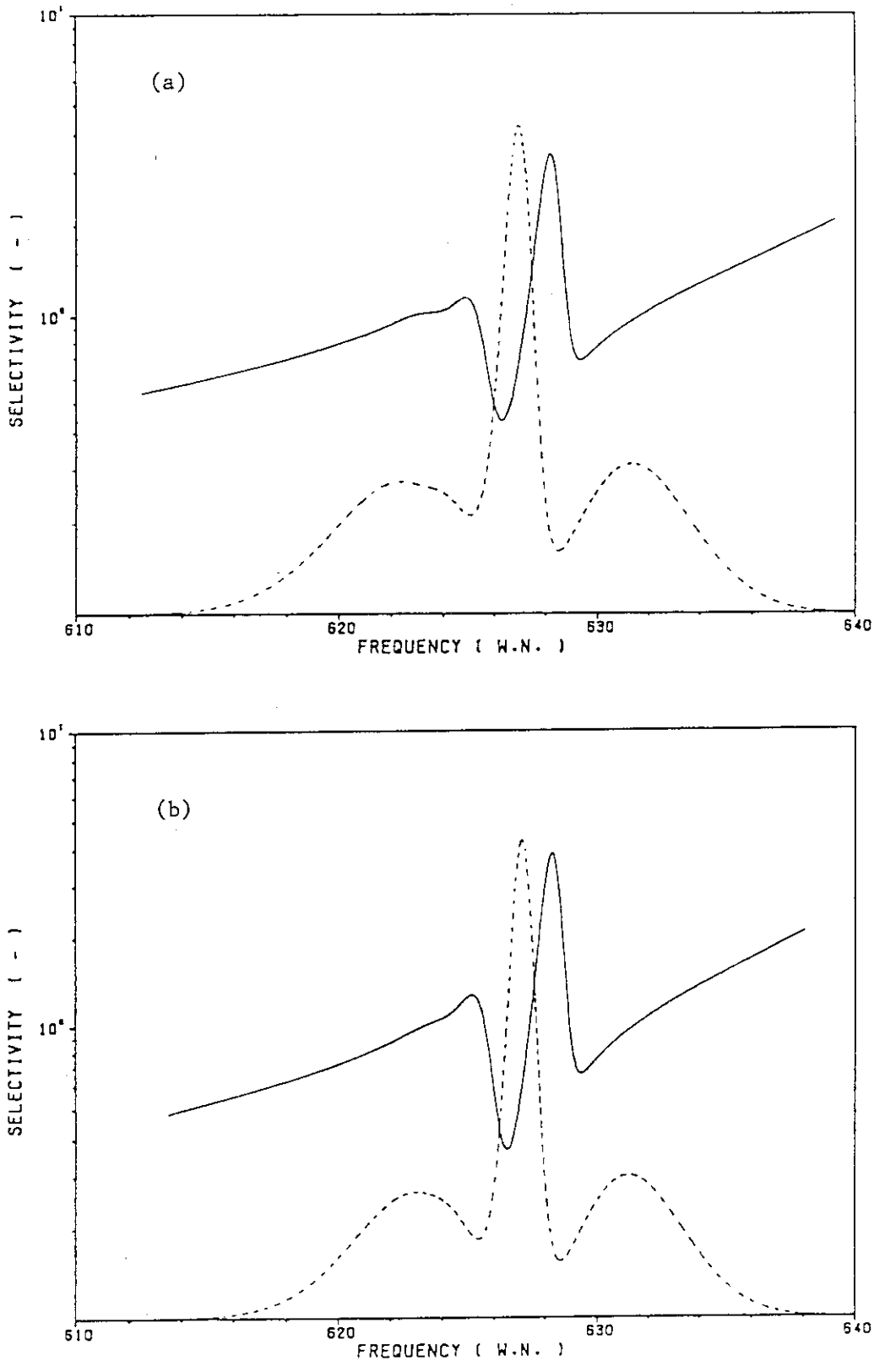

Fig.18 Isotopic selectivity as a function of absorption frequency at temperatures of (a) 200K, and (b) 170K (solid lines) compared with the ν_3 band contours (dashed lines).